Deep–Sea Research I 185 (2022) 103805

Contents lists available at ScienceDirect

Deep-Sea Research Part I

journal homepage: www.elsevier.com/locate/dsri

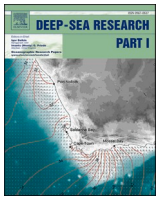

Factors influencing sea-ice algae abundance, community composition, and distribution in the marginal ice zone of the Southern Ocean during winter

Simoné De Villiërs Louw [a,*], David Richard Walker [a], Sarah E. Fawcett [b,c]

[a] Department of Conservation and Marine Sciences, Cape Peninsula University of Technology, Cape Town, South Africa
[b] Department of Oceanography, University of Cape Town, Cape Town, South Africa
[c] Marine and Antarctic Research Centre for Innovation and Sustainability (MARIS), University of Cape Town, Cape Town, South Africa

ARTICLE INFO

Keywords:
Sea-ice
Algae
Southern ocean marginal ice zone
Nutrients
Diatoms
Winter

ABSTRACT

Microalgae and bacteria living in Antarctic sea-ice play a fundamental role in polar-ocean biogeochemistry, accounting for ~25% of primary production in sea-ice-covered regions of the Southern Ocean. However, a paucity of measurements in the marginal ice zone (MIZ), particularly during winter, means that sea-ice algal dynamics are poorly understood, resulting in uncertainties in the drivers of Antarctic food-web and carbon-cycle variability. We investigated the relationships among biogeochemical parameters and sea-ice algae in the MIZ of the Indian Southern Ocean in winter 2017 through measurements of sea-ice algae functional groups, chlorophyll, and nutrient concentrations, in the sea-ice and the underlying surface seawater. We observed an abundant, active algal community within the sea-ice, which we attribute to passing cyclones that kept the ice permeable, along with biogeochemical and irradiance conditions that allowed for algal growth. The sea-ice conditions facilitated the proliferation of sea-ice diatoms, to chlorophyll concentrations >5 μg/L (versus 1.5 μg/L in the underlying seawater). The dominant taxa were of the genera *Fragilariopsis, Pseudo-nitzschia, Coscinodiscus*, and *Chaetoceros* spp., similar to those observed previously near east Antarctica. While sea-ice algae growth should have caused significant nutrient drawdown, nitrate concentrations were higher in the ice than in the underlying seawater. Since silicate was strongly drawn down, presumably by sympagic diatoms, we attribute the elevated nitrate concentrations to an active microbial loop (i.e., regeneration and nitrification). Our study highlights the ecological significance of the Southern Ocean MIZ in winter, providing a vital environment for overwintering sea-ice algae and bacteria that remain active despite the harsh conditions.

1. Introduction

The Southern Ocean (SO) plays a critical role in climate regulation (Sarmiento and Toggweiler, 1984; Siegenthaler and Wenk, 1984; Chapman et al., 2020), accounting for ~40% of the atmospheric CO_2 absorbed by the global ocean (Frölicher et al., 2015; Gruber et al., 2019). Oceanic CO_2 absorption and storage are facilitated by the solubility pump, which is the driven by the temperature dependence of CO_2 solubility and the global overturning circulation that transports CO_2 to depth, and the biological pump, which involves the fixation of atmospheric CO_2 into biomass during photosynthesis and the subsequent transport of some of this biomass into the deep ocean (Volk and Hoffert, 1985). In addition, Antarctic pack ice contributes directly to atmospheric CO_2 removal, representing an annual CO_2 sink of approximately 0.03 Pg C (>50% of the SO CO_2 sink south of 50°S) (Delille et al., 2014).

Sea-ice formation in the autumn and winter SO drives mixed-layer deepening and the resultant entrainment of nutrients into surface waters. Sea-ice melt in spring and summer subsequently stratifies the upper water column, exposing phytoplankton to sufficient light to begin consuming the entrained nutrients, thereby driving the biological pump. SO sea-ice algae also contribute to the biological pump via the seeding of sea-ice-edge blooms in the marginal ice zone (MIZ) (Szymanski and Gradinger, 2016; Yoshida et al., 2020), which is defined as the transition zone between the open (ice-free) ocean and dense pack ice. These blooms account for approximately 50% of total MIZ primary production, yet the composition of the responsible sympagic and/or pelagic phytoplankton communities is still debated (Yoshida et al., 2020). Along with their well-known contributions to regional biogeochemical processes (e.g., the biological pump, ecological stoichiometry, and the sulphur cycle; Kettle et al., 1999; Kang et al., 2001; Nair et al., 2015; Tréguer et al.,

* Corresponding author. Cape Peninsula University of Technology, Cape Town, South Africa.
E-mail addresses: 215118677@mycput.ac.za, simonelouw95@gmail.com (S.D.V. Louw).

https://doi.org/10.1016/j.dsr.2022.103805
Received 5 December 2021; Received in revised form 8 May 2022; Accepted 13 May 2022
Available online 17 May 2022
0967-0637/© 2022 Elsevier Ltd. All rights reserved.

2018; Goto-Azuma et al., 2019), phytoplankton and sympagic algae also serve as a primary energy source for higher trophic levels such as zooplankton and fish (Kohlbach et al., 2018). The transfer of carbon to higher trophic-level pelagic organisms in the SO is especially important in winter when primary production in polar waters is assumed to be near-zero (Kohlbach et al., 2018).

Antarctic sea-ice is a heterogenous environment characterized by ephemeral physical properties (McMinn, 2017; Yoshida et al., 2020). Sea-ice algae that aggregate within the ice experience extreme fluctuations in light, temperature, pH, and nutrient and gas (e.g., CO_2 and O_2) concentrations (McMinn, 2017), which influence their photosynthetic efficiency, production, and physiology. The MIZ is an ideal environment in which to investigate the sea-ice algae species that can withstand abiotic and biotic co-stressors, both within the sea-ice and in the pelagic environment, either as phytoplankton cells or as resting spores. The biogeochemical and physical properties of SO winter sea-ice are currently under-sampled (Sambrotto et al., 2003; Fripiat et al., 2017; Tison et al., 2020), in part because of the logistical challenge associated with wintertime sampling, and phytoplankton community response (e.g., photo-physiology and biomass) to changing sea-ice morphology which is sparsely documented (Torstensson et al., 2018). This lack of data, in turn, results in the potentially erroneous representation of ecological communities (e.g., phytoplankton assemblages in biogeochemical or ecological models) and a poor understanding of their significance for SO ecosystem functioning, nutrient cycling, and CO_2 removal (Bouman et al., 2012; Chapman et al., 2020).

Each diverse bioregion surrounding Antarctica is already being impacted by environmental stressors associated with climate change (Deppeler and Davidson, 2017; Henley et al., 2020). The short and medium-term effects of climate change on sea-ice extent are likely to alter trophic food-web interactions and the release of organic material and nutrients (e.g., iron) during seasonal sea-ice melt (Brierly and Thomas, 2002; IPCC SROCC et al., 2019). As for the broad trends observed across the polar SO, sea-ice extent increased in the Weddell Sea and Indian Ocean regions between the late 1970s and 2014 (Parkinson, 2019). Thereafter, a rapid decrease occurred, with sea-ice extent reaching a record low in 2017. Investigating MIZ ecosystem functioning during this period (austral winter 2017) and in this location (Southern Indian MIZ) could provide useful information on plankton community response to declining sea-ice extent, particularly as this trend is predicted to continue in future (Rackow et al., 2020).

Climate-induced stressors are predicted to impact phytoplankton community productivity and composition in most SO bioregions (Deppeler and Davidson, 2017; Pinkerton et al., 2021). As such, it is reasonable to anticipate changes in SO carbon export, biogeochemistry, and trophic food web structure (Henley et al., 2020; Morley et al., 2020). The eco-physiological response of phytoplankton to environmental change will be taxon-specific and likely includes the ability to adapt (Lacour et al., 2017). Before we can fully understand how climate change will influence the ecological functioning of phytoplankton taxa in sympagic and pelagic ecosystems, however, we require more data on the current functioning of sea-ice algae communities. In this study, we investigated the taxonomic composition and abundance of sea-ice algae and the surrounding pelagic phytoplankton community in the MIZ of the Indian SO during the austral winter of 2017. The sympagic and surrounding surface water (<5 m depth) physicochemical environments (nutrients, temperature, and salinity) were also characterized in an attempt to assess the drivers of sea-ice algae community structure and abundance.

2. Methodology

2.1. Study area

Sea-ice samples were collected during austral winter (July) 2017 in the MIZ of the Indian sector of the SO at 65°S, 30°E (Fig. 1) onboard the R/V *SA Agulhas II* (VOY25). The MIZ edge was defined by 30% ice cover and was encountered at 61.7°S (De Jong et al., 2018). The MIZ was covered in first year ice, including 50% pancake floes between 2 and 4 m in diameter that were approximately 40 cm thick, with frazil ice filling the interstitial gaps (Vichi et al., 2019). Unlike the Antarctic continent, which experiences 24 h of darkness in winter (Clark et al., 2013; Núñez-Pons et al., 2018), the photoperiod in the MIZ during our study was approximately 6 h, similar to that recorded during austral winter in

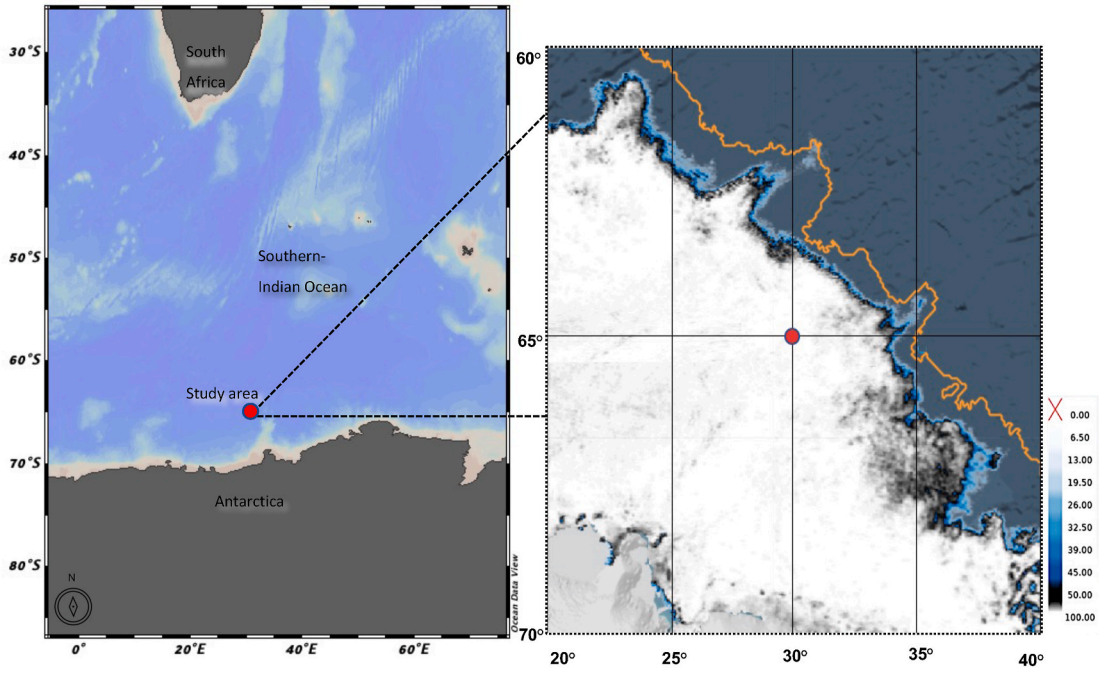

Fig. 1. Left: Map of the sampling location (sea-ice and seawater) in the Southern Ocean's marginal ice zone (red dot). **Right:** Sampling location in the context of average sea-ice concentration (colours) and median sea-ice extent (orange line) for the 3rd of July 2017 (map extracted from meereisportal.de).

the South Atlantic MIZ (SCALE project, Skatulla et al., 2021) and the Weddell-Scotia Sea MIZ (between 7.1 and 8.6 h; Cota et al., 1992). Solar irradiance in the SO is highly seasonal, with fluxes of 0–800 μmol photons m^{-2} d^{-1} recorded in austral spring, summer, and winter (Cota et al., 1992; Lazzara et al., 2007; Hoogstraten et al., 2012). Moreover, during cloud free days, instantaneous irradiance above the sea surface has been known to reach 1200 μmol photons m^{-2} d^{-1} in the MIZ in winter (Cota et al., 1992). The optical properties and thickness of snow cover and the sea ice itself can also influence irradiance levels within the ice (Eicken, 1992). The pancake floes were covered with a negligible amount of snow (0–2 cm), comparable to previous observations from the MIZ (Lizotte and Sullivan, 1991; Skatulla et al., 2021).

Three individual ice samples ("pancakes") were collected using a sampling apparatus (a spreader beam structure bearing a 5 m × 5 m heavy-duty net) designed by the Engineering Department at the University of Cape Town. While care was taken to preserve the integrity of the ice samples, our method of pancake collection could have resulted in some brine drainage, possibly modifying the sea-ice salinity and biogeochemical profiles. The pancakes were approximately 1 m in diameter and were collected at night to avoid light exposure. Two of the ice samples were cut into three vertical and four horizontal segments using an electric band saw, yielding 12 cubes of 10 cm^3 for each pancake. The third pancake was divided into four vertical and four horizontal segments, for a total of 16 cubes of 10 cm^3. Each cube was melted in the dark at room temperature, then subsampled for chlorophyll-a and nutrient analysis, and microalgae identification. Two surface seawater samples were collected from <5 m depth near (within ~5 m of) the sea-ice samples using a Conductivity-Temperature-Depth (CTD) rosette sampler equipped with an array of Niskin bottles. The seawater samples were similarly processed for chlorophyll-a, nutrients, and microalgae taxonomy.

2.2. Sea-ice algae species composition

Melted sea-ice samples (400 mL) for algae identification were preserved with 2.5 mL of Lugol's iodine solution (2% final concentration) and stored in amber bottles at low room temperature (20 °C) away from direct sunlight on board the R/V *SA Agulhas II*. At the Cape Peninsula University of Technology ecotoxicology laboratory, the sea-ice samples were settled using the Utermöhl method (Utermöhl, 1931), by which 20 mL of sample was left to settle onto a coverslip for 24 h. Microalgae species were then counted and identified using an inverted light microscope (Olympus CKX41) at a magnification of 100× to 200×.

Forty mL of the three melted sea-ice samples containing the most diverse species assemblages were further analysed using Scanning Electron Microscopy (SEM). Samples were filtered onto Whatman 0.2 μm Nucleopore track-etch membrane filters and left to dry for ~12 h in a petri dish. These were analysed at the Iziko South African Museum Marine Biology Department using a Hitachi T4000 Plus Table-top SEM with images viewed at 5 kV using backscatter electrons.

Identification of taxa from light microscopy and SEM was carried out following Scott and Marchant (2005). A total of 48 sea-ice algae taxa were identified, but due to the limited microscope resolution, some could not be reliably discriminated to species level. Therefore, the following algae groups were characterised to genus level: *Fragilariopsis* spp., *Pseudo-Nitzschia* spp., and *Nitzschia* spp., while others were identified to species level where possible.

2.3. Chlorophyll-a analysis

Sea-ice and surface seawater samples were analysed shipboard for chlorophyll-a concentrations. Aliquots of melted sea-ice and seawater were filtered through 0.3 μm (100 mL) and 2.7 μm (500 mL) glass fibre filters (GF-75s; Sterlitech) that were then extracted in 8 mL of 90% acetone for 24 h at −20 °C. The fluorescence of the extracted sample was measured using a Turner Designs Trilogy fluorometer, and fluorescence was converted to chlorophyll-a following the non-acidified method of Welschmeyer (1994). The fluorometer was calibrated with a Sigma-Aldrich® chlorophyll-a analytical standard (*Anacystis nidulans*) prior to and after the cruise.

The size-fractionated chlorophyll-a measurements were used to classify sea-ice algae cells as either pico-plankton or large algae cells. Large algae cells were classified as the cell fraction >2.7 μm (i.e., micro and nano-plankton). Pico-plankton biomass was calculated by subtracting the chlorophyll of the large algae cells from the total chlorophyll (>0.3 μm), which yields a measure of the 0.3–2.7 μm fraction.

2.4. Nutrient analysis

Standard spectrophotometric and fluorometric methods were used to determine the nutrient concentrations in each cube of pancake ice and in the underlying seawater (Grasshoff et al., 1983; Holmes et al., 1999). Ice and seawater samples were filtered immediately after melting using a 0.2 μm syringe filter, with approximately 50 mL of liquid decanted into a clean polypropylene tube for nitrate, nitrite, silicate, and phosphate analysis; samples were frozen at −20 °C until analysis ashore. Additionally, 40 mL of 37 sea-ice samples (pancake 2 and underlying seawater) were collected in "aged" (i.e., stored with Milli-Q + working reagent; Smith et al., 2021) high-density polyethylene bottles for shipboard ammonium concentration analysis.

The non-ammonium nutrient samples were analyzed in the Marine Biogeochemistry Laboratory at the University of Cape Town following the cruise. A Latchet Quick-Chem flow injection autoanalyzer was used to determine nitrate+nitrite and silicate concentrations following published auto-analysis protocols (Grasshoff, 1976; Diamond, 1994). Nitrite and phosphate were determined manually using the colorimetric methods described by Grasshoff et al. (1983) and a Thermo Scientific Genesis 30 Visible spectrophotometer. Precision of the nitrate, silicate, nitrite, and phosphate measurements was ±0.18 μM, ± 0.04 μM, ± 0.08 μM, and ±0.11 μM, respectively, while the detection limit was 0.1 μM, 0.2 μM, 0.05 μM, and 0.05 μM, respectively. Aliquots of a certified reference material (JAMSTEC) were analysed during autoanalyzer and manual runs to ensure measurement accuracy.

Ammonium concentrations were measured shipboard according to the fluorometric method of Holmes et al. (1999) using a Turner Designs Trilogy fluorometer equipped with a UV module. Precision was ±0.05 μM and the detection limit was <0.05 μM. The matrix effect (ME) was calculated using the standard addition method (Saxberg and Kowalski, 1979) and an ME correction, typically ≤5%, was applied to all samples (Taylor et al., 2007). Hereafter, all references to total nitrogen (N) are to nitrate+nitrite; ammonium concentrations were not added to the total N pool because we do not have ammonium data for all the pancakes.

To account for the physical effects of temperature-driven concentration and/or dilution in the sea ice, which causes nutrient distributions in the brine to change during melting or freezing, salinity-normalised nutrient concentrations are typically used (Gleitz et al., 1995; Thomas and Dieckmann, 2002a and references therein; Papadimitriou et al., 2007; Fripiat et al., 2017). We calculated salinity-normalised nutrient concentrations according to the method outlined by Fripiat et al. (2017). Briefly, nutrient concentrations were normalised to the underlying seawater salinity as: Normalised sea-ice nutrient concentration = measured sea-ice concentration x (seawater salinity/sea-ice salinity). Hereafter, all references to sea-ice nutrient concentrations are to the salinity-normalised values.

2.5. Temperature and salinity analysis

Temperature was recorded immediately after sea-ice collection by inserting an electric thermometer into the centre of each cut pancake segment. After the ice samples were melted, a Portasal 8410A salinometer was used to measure salinity shipboard according to standard procedures outlined by Guildline Instruments (1981) and UNESCO

(1978). The salinometer was operated at a 23 °C bath temperature and 21 °C ambient laboratory temperature, and was regularly calibrated using IAPSO Seawater Standards (OSIL). Seawater temperature and salinity were measured using a Seabird CTD sensor package (SBE 911), with CTD-derived salinity verified by comparison with direct measurements.

Brine volume (V_b) was computed using the sea-ice temperature and salinity measurements according to the method outlined in Cox and Weeks (1983). Briefly, sea-ice salinity (S_i) and density (ρ_i) were divided by the brine salinity (S_b) and density (ρ_b) at the temperature of interest and multiplied by the sea-ice sample volume (V_i): $V_b/V_i = p_i.S_i/p_b.S_b$.

2.6. Statistical analysis

The algal community and biogeochemical environment were statistically analysed using 42 samples (40 sea-ice and 2 surface-water data points). According to the Central Limit Theorem (CLT), a sample size of more than 30 data points is usually sufficient for statistical analysis (Dodge, 2008). The species community were analysed using univariate and multivariate statistical approaches. A multivariate analysis was done using the PRIMER v6 statistical package together with the PERMANOVA Plus package (Clarke and Gorley, 2006; Anderson et al., 2008). Data were fourth-root transformed and converted to a similarity matrix using the Bray-Curtis similarity coefficient. A one-way permutational multivariate analysis of variance (PERMANOVA) was used to test the homogeneity of variance ($p < 0.05$) of the sea-ice algae (including all protist functional groups: diatoms, dinoflagellates, silicoflagellates, coccolithophores, and ciliates) community structure, biomass (chlorophyll-a), and nutrient concentrations according to discrete sea-ice depth layers and pancake samples. The similar percentage routine (SIMPER) using Bray-Curtis distance was used to identify species contributing the most towards (dis)similarity in community composition across depth layers (shown as species contribution and average abundance).

Standard diversity indices were calculated according to sea-ice depth layer as follows: the Shannon Wiener diversity index (H′), $H' = \Sigma_i\ p_i(\ln p_i)$, where p_i is the proportion of the total sample represented by a particular species (i.e., the number of individuals in a species divided by the total number of individuals in the community) (Hayek and Buzas, 2013), and species evenness (Pielou's J′) was determined using $J' = H'/H'max = H'/\ln S$, where H'max is the maximum possible value of Shannon diversity (InS) and S is the total number of species (Clarke and Warwick, 2001). Species richness was determined according to Margalef's index as $d = (S-1)/\ln N$, where N is the number of individual cells (Clarke and Warwick, 2001).

A hierarchical clustering analysis and non-metric multidimensional scale plot (MDS) were used to derive a proximity matrix indicating the similarity of species community assemblages relative to their position (Clarke and Warwick, 2001). The MDS plot illustrates the "natural algae groupings" according to sea-ice depth layer and individual samples.

A Distance Based Linear Model (DistelM) was used to explain the relationship between biological variations and nutrient concentrations using the PERMANOVA Plus package. The DistelM partitioned the variation in the biological data according to a multiple regression model (based on the parameters depth-layer, sample, and the interaction between depth-layer and sample) using the R^2 function as a stepwise procedure.

The IBM SPSS 26 statistics package was used to derive relationships between sea-ice algae community abundance and biogeochemical sympagic variables (nutrients and chlorophyll-a). To test homogeneity of variance among sea-ice samples, a multivariate analysis by combined dependent variables was used. No significant difference between variables was identified, as per Pillai's trace p-value. The Shapiro Wilkinson normality test was used to verify the equality of variances of sea-ice algae abundance in sea-ice samples. A Spearman's rank-order correlation coefficient was computed to determine the strength of the monotonic relationship between environmental variables and sea-ice protist functional groups (diatoms, dinoflagellates, silicoflagellates, coccolithophores, and ciliates). Significance levels for all statistical tests were taken to be $p < 0.05$.

3. Results

3.1. Physical and biogeochemical environment

All three pancakes contained a brine volume >5% at each sample depth (Fig. 2a). Salinity was low, ranging between 2 and 6‰, and showed no distinct trend with depth in the pancakes (i.e., profiles were fairly isohaline; Fig. 2b). Similarly, sea-ice temperature ranged between −2 and −1 °C and showed a largely isothermal profile (Fig. 2c).

In the sea-ice, the nitrate (NO_3^-) and silicate ($Si(OH)_4$) concentrations averaged 33.7 ± 37.2 μM and 33.6 ± 35.3 μM, respectively, and no clear trend was evident with pancake depth-layer (Fig. 3a). The phosphate (PO_4^{3-}), nitrite (NO_2^-), and ammonium (NH_4^+) concentrations were lower, averaging 1.3 ± 2.6 μM, 1.2 ± 2.6 μM, and 2.6 ± 7.7 μM, respectively (Fig. 3b). Nitrogen ($N = NO_3^- + NO_2^-$) and $Si(OH)_4$ were significantly correlated ($p < 0.05$, $R^2 = 0.66$), and a fairly constant N:Si $(OH)_4$ molar ratio of ~1:1 was observed for all sea-ice samples (Fig. 4a and b). Nitrogen-to-phosphate (N:P) ratios were variable, ranging between 0 and 120:1 and averaging 27.4:1, with a median of 21.8:1 (Fig. 4c). No correlation ($R^2 = 0.005$) was observed between N and PO_4^{3-} (Fig. 4d). In the sea-ice, ammonium concentrations decreased from top to bottom, with an average concentration of 7.7 μM in the top layer and values <3 μM in the bottom layer (Fig. 3b). In the surrounding surface seawater, the concentrations of the nitrogen species were notably lower ($NH_4^+ = 0.70$ μM, $NO_3^- = 26.9$ μM, and $NO_2^- = 0.23$ μM) than in the sea-ice (Fig. 3a and b). In particular, nitrate was on average 6.4 ± 7.8 μM higher in the sea-ice than in the seawater. Conversely, silicate concentrations were higher in the surface water (46.7 μM) than in the sea-ice (average of 33.8 ± 37.2 μM), while phosphate concentrations were similar between the surface waters and the sea-ice (average of 2.0 μM and 1.3 ± 2.6 μM, respectively). The N:$Si(OH)_4$ ratio of the seawater was 1:1.7 and the N:P ratio was 13.4:1.

Salinity and nutrient concentrations were generally not significantly correlated, at the level of both the individual pancake samples and at discrete depths. Ammonium concentrations, however, increased significantly with decreasing salinity in pancake 2. According to the two-way PERMANOVA, nutrient concentrations were significantly different (p (perm) < 0.001) in individual pancake samples, but not with depth.

3.2. Sea-ice algae biomass

Average total sea-ice algae biomass (represented by total (>0.3 μm) chlorophyll-a) was significantly ($p < 0.05$) higher than that measured in surface waters (average of 1.16 ± 3.14 μg/L versus 0.14 ± 0.15 μg/L) and reached a maximum in the interior of the pancakes (Fig. 5a; average of 4.13 and 4.64 μg/L). Larger sea-ice algae (>2.7 μm) dominated the chlorophyll-a biomass in all depth layers (82 ± 90% on average). Significant differences ($p < 0.05$) were found between individual pancake samples and between the top and interior depth layers in pancake 2.

3.3. Biological community structure

Sea-ice algae cell abundance was significantly ($p < 0.01$) higher in the sea-ice (6076–14730 cells/mL) compared to the surrounding surface seawater (23–473 cells/mL) (Table 1), with the highest cell concentrations generally observed in the interior of the pancakes (Fig. 5b and c). Diatoms represented the dominant functional group in both the sea-ice and the underlying surface water (diatoms, both pennate and centric, contributed 92.7% and 99.6% of the total algal cell abundance in the sea-ice and underlying surface water, respectively; Fig. 5b and c).

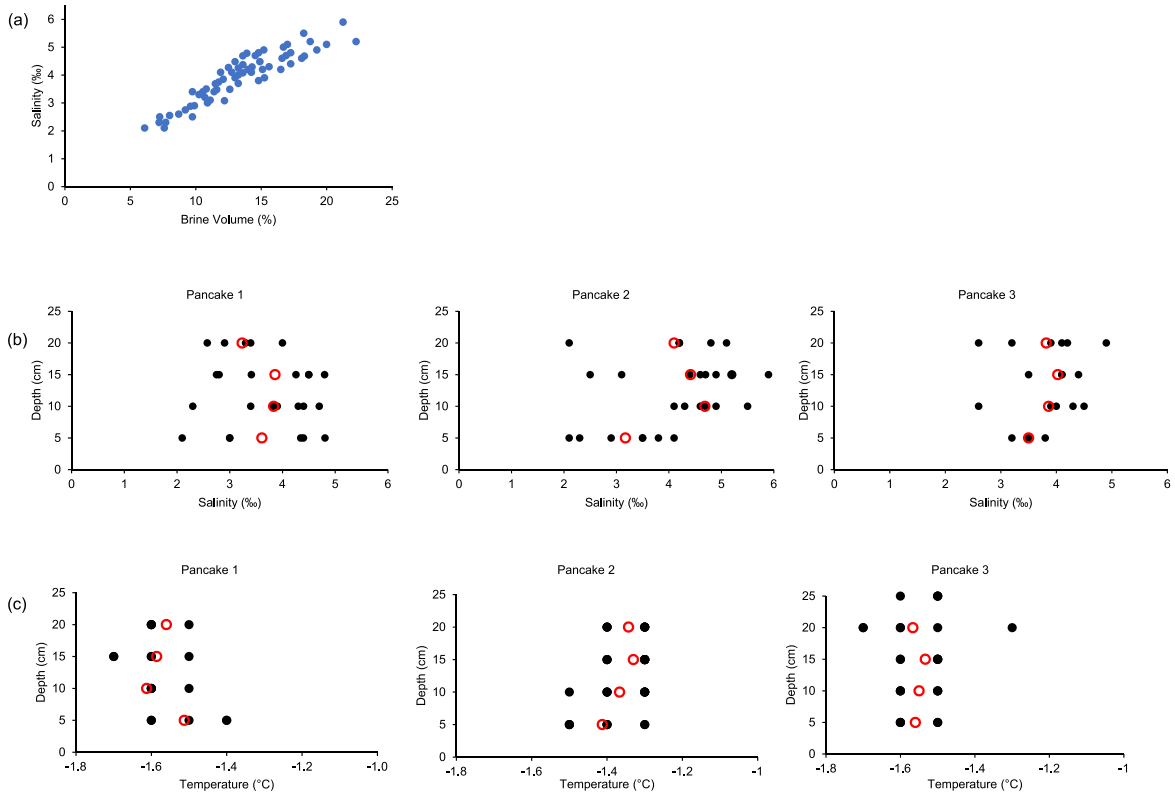

Fig. 2. Vertical pancake-ice profiles of physicochemical parameters: (a) brine volume (%), (b) salinity (‰), and (c) temperature (°C). Red circles indicate the average salinity (‰; panel b) and temperature (°C; panel c) at each depth.

Pennate diatoms dominated all layers, often exceeding concentrations of 600 cells/mL, while centric diatom concentrations were much lower. Centric diatom abundance was nonetheless higher than that of the other main protist groups (silicoflagellates, coccolithophores, dinoflagellates, and ciliates), exceeding 26 cells/mL in all sea-ice depth layers whereas the other protists rarely reached 20 cells/mL (Fig. 5b and c). Compared to the surrounding surface water, sea-ice centric diatom abundance was low (average centric diatom abundance of 33.6 ± 87.7 cells/mL in the sea-ice (median of 60.1 cells/ml) and 92.6 cells/mL in surface waters) while sea-ice pennate diatom abundance was higher than in the surrounding seawater (average of 440.2 ± 790.4 cells/mL and 9.62 cells/mL, respectively). In the sea-ice, the ciliates, silicoflagellates, and coccolithophores were present at higher average abundances than the dinoflagellates (Fig. 5c), and the non-diatom protist community showed no distinct abundance pattern according to depth layer. However, coccolithophores were generally more abundant than the other groups, and mostly concentrated in the bottom layer (except in pancake 2). Conversely, in the surface seawater, dinoflagellates were more abundant than the other protist groups, with the latter either absent or present at very low abundances (~2 cells/mL) (Table 1 and Fig. 5c).

No clear pattern emerged for the diversity indices (species richness and diversity) in the sea-ice samples (Table 2). The sea-ice protist community (i.e., all microalgae groups) was mostly unevenly distributed (Pielou's J' <0.5) in all depth layers. This result suggests that in each sea-ice depth layer, one or more taxa dominated the species community structure in terms of abundance. Diatoms of the pennate genus *Fragilariopsis* dominated the sea-ice protist community, showing the highest average abundance across all depth layers (Table 2). Additionally, this genus was responsible for most of the similarity in community structure among the top (20%), interior (22%), and bottom (25%) layers. Other dominant pennate diatoms found across all depth layers were identified as *Pseudo-nitzschia* spp. and *Proboscia* spp. The dominant centric diatoms were *Chaetoceros* spp., *Chaetoceros dichaeta*, and *Coscinodiscus* spp., which generally contributed significantly across all depth layers. A markedly lower abundance of *Dactyliosolen antarcticus*, a diatom species of the class *Coscinodiscophyceae*, was observed in the top layers than deeper in the pancakes. By contrast, *Corethron* spp. contributed >90% of the (dis)similarity in the top layer, in contrast to the interior and bottom layers (Table 2). More broadly, however, average dissimilarity was low (37%) between pancake depth layers, indicating that the same species were present in each depth layer.

Significant differences ($p < 0.001$) in algal community composition among discrete samples, depths, and depth × sample interaction were indicated by the PERMANOVA. The MDS analysis showed distinct groupings in community structure according to depth and pancake (Fig. 6a). Here, the top layers were generally closely correlated (pancake 1 and 3), while the interior and bottom layers tended to group together. These groupings are in agreement with significant differences among depth layers insofar as no significant difference was found between the bottom and interior layers of the pancake samples. According to the MDS, community structure in the surface seawater was markedly different from that in the sea-ice.

3.4. Relationship between the biogeochemical sympagic environment and algae community structure

Several significant relationships ($p < 0.05$) emerged between nutrient concentrations and sea-ice algae biomass (i.e., chlorophyll-a) when the pancakes were tested without considering depth layers (Table 3). Overall, pico-sea-ice algae biomass (0.3–2.7 μm) was significantly negatively correlated with both nitrate and silicate concentrations. When sea-ice depth layers were individually tested, additional significant relationships ($p < 0.05$) emerged (Table 3): the interior layer was characterized by a negative correlation between pico-sea-ice algae biomass and both nitrate and silicate concentration, as well as between nitrite concentration and total chlorophyll-a; and a positive correlation

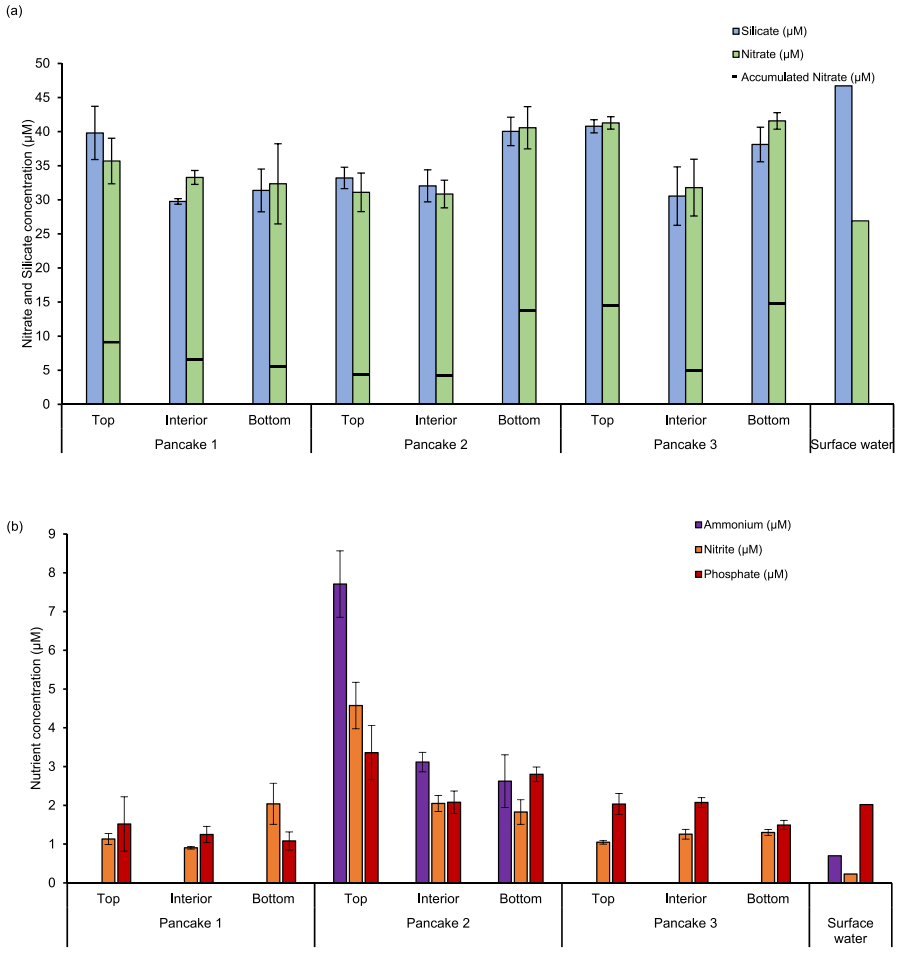

Fig. 3. Average concentrations (µM) of (a) nitrate and silicate and (b) nitrite, phosphate, and ammonium in the pancake sea-ice according to depth layers, and in the surface seawater associated with the pancake ice. Vertical error bars denote the standard error (SE) of the mean. "Accumulated nitrate" was calculated as sea-ice nitrate concentration minus seawater nitrate concentration, and so represents the net accumulation of nitrate in the sea-ice since its formation.

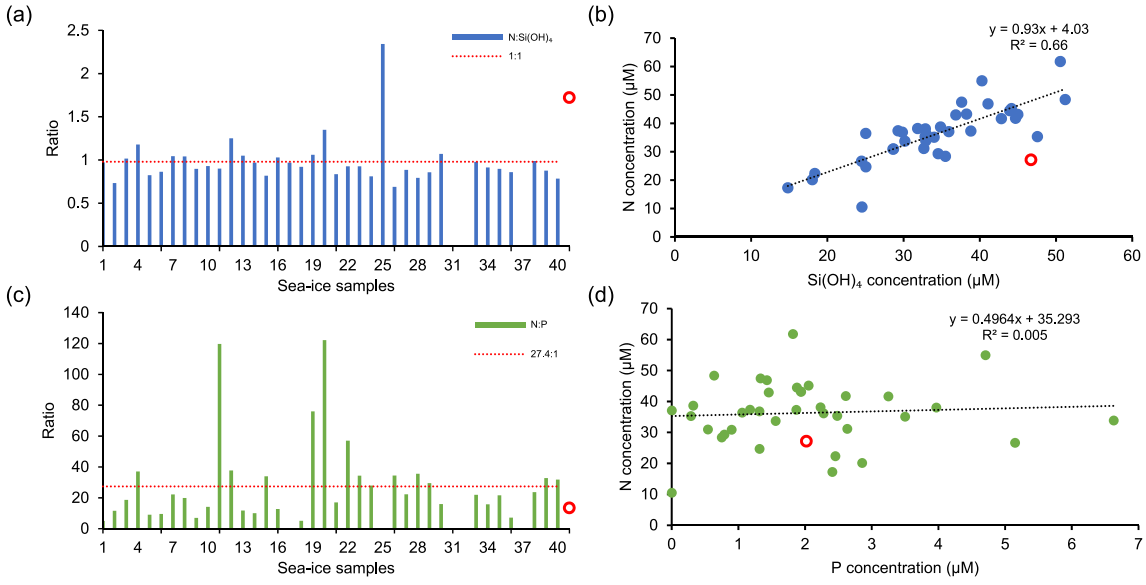

Fig. 4. Nitrogen (N) and silicate (Si) (µM) (a) molar ratio and (b) linear regression, and N and phosphate (P) (c) molar ratio and (d) linear regression for all pancake sea-ice samples. The red circles indicates the underlying surface water molar ratios (panels 4a and c) and nutrient concentrations (panels 4b and d).

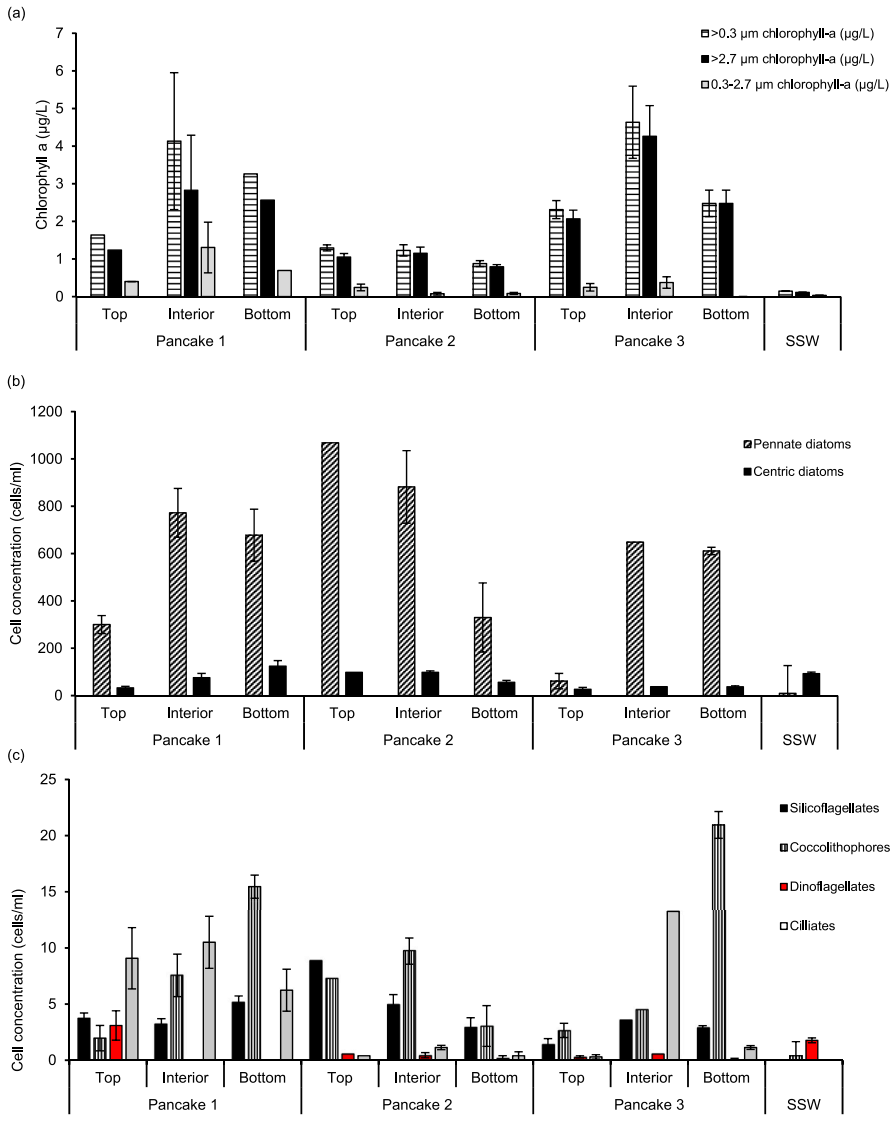

Fig. 5. Average concentration of (a) chlorophyll-a (µg/L) (for the bulk (i.e., >0.3 µm), nano- and microplankton (>2.7 µm), and picoplankton (0.3–2.7 µm) size classes), (b) diatoms (cells/mL), and (c) other protist groups (i.e., silicoflagellates, coccolithophores, dinoflagellates, and ciliates) in the pancake sea-ice samples according to depth layer, as well as in the surface seawater (SSW) associated with the pancake ice. Vertical bars denote the SE of the mean.

between pico-sea-ice algae and nitrite concentration was observed in the bottom layer.

Total sea-ice algae, pennate diatom, and silicoflagellate abundances increased significantly ($p < 0.05$) with decreasing silicate and nitrate and increasing nitrite concentrations in the top layer of all the pancakes (Table 4). The interior layer was characterized by a significant positive relationship ($p < 0.05$) of ciliate and silicoflagellate abundance to phosphate concentration. Ciliate abundance was also negatively correlated ($p < 0.05$) with nitrite concentration in this layer. The bottom layer showed significant ($p < 0.05$) negative relationships between centric diatom abundance and nitrite concentration.

The relationship between nutrient concentrations and sea-ice algae was further analyzed using a Distance Based Linear Model output (DistelM). Independently tested nutrients (nitrite) influenced the total variation of the biological community significantly ($p < 0.05$) (marginal test) (Table 5). When the cumulative effects (sequential test) of nutrient concentrations were analyzed, nitrite and silicate were the only variables with a significant impact on the total biological variation. Despite this, the nutrient concentrations do not explain the total variation of the biological community structure very well (15.9%) (Fig. 6b).

4. Discussion

4.1. Physical and biogeochemical environment

Sea-ice brine volume fraction determines sea-ice permeability, which in turn controls the mobility of biogeochemical constituents in ice (Tison et al., 2020). All sea-ice samples were permeable according to the >5% brine volume threshold (Fig. 2a; Golden et al., 1998), with the physical sea-ice structure characterized by a coalesced brine network wherein seawater (brine) could move freely (Fripiat et al., 2014). In addition, the pancake floes collected at all three sampling sites were <1 m in diameter, which indicates pancake growth via the frazil life cycle, as opposed to welding that characterizes pancake floes of larger size (>4 m) (Alberello et al., 2019). Pancake ice floes formed via the frazil life cycle have a decoupled brine channel system, with varying channel sizes that do not follow likely growth trends associated with depth layers in sea-ice (Lieblappen et al., 2018). It is thus possible that the frazil sea-ice life cycle could account for some of the differences we observe in biogeochemical properties with depth in the ice, if the accumulation of organic material and/or inorganic nutrients follows the uneven distribution of

Table 1
Protists (i.e., microalgae groups) recorded in pancake sea-ice and surface water samples (MIZ 1). Total abundance (cells/mL) is listed for taxa grouped according to phylum.

Protist community composition	Pancake 1 (cells/mL)	Pancake 2 (cells/mL)	Pancake 3 (cells/mL)	MIZ 1 (cells/mL)
Actinopoda	0	1	0	0
Phaeodaria	0	1	0	0
Phaeogromia spp.	0	1	0	0
Challengeridae spp.	0	1	0	0
Protocystis bicornuta	0	1	0	0
Bacillariophyta	8329	14730	6076	496
Diatomophyceae	8329	14730	6076	496
Biddulphiales	1263	1808	669	177
Asterolampraceae spp.	12	14	2	0
Asteromphalus hookeri	0	0	1	0
Asteromphalus hyalinus	0	8	1	0
Asteromphalus spp.	5	2	1	0
Eucampia antarcticus	8	4	0	0
Chaetocerotaceae	863	1219	281	42
Chaetoceros atlanticus bulbous	8	19	9	0
Chaetoceros convolutus	0	22	0	0
Chaetoceros criophilus	38	100	4	10
Chaetoceros dichaeta	157	161	102	0
Chaetoceros spp.	659	918	165	32
Coscinodiscaceae	143	136	125	10
Coscinodiscus spp.	143	136	125	10
Heliopeltaceae	2	0	0	0
Actinoptychus senarius	2	0	0	0
Hemidiscaceae	0	2	0	0
Actinocyclus spp.	0	2	0	0
Leptocylindraceae	31	30	14	0
Corethron spp.	8	21	7	0
Leptocylindrus danicus	23	9	7	0
Rhizosoleniacceae	145	223	124	10
Dactyliosolen antarcticus	96	126	54	6
Guinardia spp.	8	20	9	0
Proboscia spp.	37	75	59	4
Rhizosolenia spp.	4	3	2	0
Unknown centrics	67	184	122	113
Bacillariales	7052	12892	5386	317
Bacillariaceae	6859	12615	5119	315
Cylindrotheca closterium	18	36	2	8
Fragilariopsis kerguelensis	52	246	103	6
Fragilariopsis spp.	6656	12016	4892	292
Nitzschia spp.	0	12	0	0
Pseudo-nitzschia delicatissima	38	4	72	0
Pseudo-nitzschia spp.	95	302	49	9
Fragilariaceae	1	23	0	0
Thalassiothrix antarctica	1	23	0	0
Naviculacceae	28	75	50	2
Membraneis challengeri	0	2	0	0
Navicula glaciei	2	0	7	0
Navicula spp.	26	42	38	2
Pleurosigma spp.	1	0	5	0
Unknown species 1	0	31	0	0
Unknown pennates	164	179	216	0
Unknown diatoms	14	29	22	2
Ciliophora	103	12	59	1
Spirotrichea	0	2	0	0
Tintinnida	0	2	0	0
Xystonellidae	0	2	0	0
Cymatocylis spp.	0	2	0	0
Unknown ciliates	103	11	59	1
Haptophyta	100	119	112	0
Haptophyceae	100	119	112	0
Coccolithophores	100	119	112	0
	100	119	112	0
Unknown coccolithophores	48	87	32	1
Ochrophyta	48	87	32	1
Dictyochophyceae	48	87	32	1
Dictyochales	48	87	32	1
Dictyochaceae	47	84	32	1
Dictyocha speculum	2	3	0	0
Unknown silicoflagellates	12	7	4	4
Pyrrophyta	12	7	4	4
Dinophyceae	11	7	4	0
Dinophysales	1	0	0	0
Amphisoleniaceae	1	0	0	0
Dinophysis antarctica	1	0	0	0
Gymnodiniales	1	0	0	0
Gymnodiniaceae	1	0	0	0
Gymnodinium spp.	1	0	0	0
Peridinales	1	0	0	0
Protoperidiniaceae	1	0	0	0
Protoperidinium spp.	10	7	4	4
Unknown dinoflagellates	2	2	0	0
Sarcomastigophora	2	2	0	0
Granuloreticulosea	2	2	0	0
Foraminifera	2	2	0	0
Unknown foraminifers				

brine channels and pockets.

Steep nutrient gradients were generally not observed in the sea-ice in this study (Fig. 3). Additionally, salinity was near homogenous through the ice, with no clear distinction between depth layers (Fig. 2b). These isohaline profiles were likely cause by the fairly-high permeability of the sea-ice structure and the cyclonic storm conditions that caused flooding of the sea-ice surface during the sampling period (1–4 July 2017). At the time of sampling, Vichi et al. (2019) recorded several cyclones, including an explosive extratropical cyclone, crossing the South Atlantic MIZ; these systems are expected to influence the fluid flow, biogeochemical properties, and micro-structure of the sea-ice, especially at its surface. Although it has been postulated that brine behavior largely regulates the inorganic nutrient pools in newly formed sea-ice, (Vancoppenolle et al., 2010), salinity and nutrient concentrations (nitrate, silicate, nitrite, and phosphate) were not significantly correlated in our study, suggesting that brine drainage was not a major driver of our observations. Such a lack of correlation between salinity and nutrients tends to occur after ice ages or over complete seasons due to a prolific biological community (Dieckmann et al., 1991; Fripiat et al., 2017). It is thus possible that the pancakes hosted an active sympagic biological community that actively altered the distribution of nutrients within the ice, decoupling the salinity and nutrient concentrations (Vancoppenolle et al., 2010).

We recorded a higher accumulation of algal cells (abundance and chlorophyll-a biomass) in the sea-ice compared to the surrounding surface seawater (Fig. 5a). This observation suggests either the passive accumulation in forming sea-ice of algal material derived from surface seawater or that some sea-ice algae species were actively growing in the ice during the winter. The negative correlations between total protist abundance (i.e., all microalgae groups) and the nitrate and silicate concentrations (Table 4) strongly suggest active nutrient consumption by sea-ice algae, which is anticipated for a growing sea-ice algae community (Wetzel, 2001). Additionally, the near-constant N:$Si(OH)_4$ ratio of 1:1 measured in most sea-ice samples (Fig. 4a), and the significant positive correlation ($p < 0.05$, $R^2 = 0.66$) between nitrate and silicate, the concentrations of which changed in a ratio of 1:1 (Fig. 4b), evince active biogeochemical processes occurring during or prior to our sampling. First, the N:$Si(OH)_4$ ratio in surface seawater at the time of

Table 2
Sea-ice algae species that contributed most towards similarity across pancake sea-ice depth layers (% calculated using SIMPER). "Avg. Abund" refers to average cell abundance while "Contrib" refers to percent contribution. Average dissimilarity across all groups was 36.6%. Species that contributed <90% to total community abundance are denoted [A]. Average diversity indices (Margalef d and Pielou's J′) were computed across sea-ice depth layers.

	Top		Interior		Bottom	
	Avg. Abund (cells/mL)	Contrib. (%)	Avg. Abund (cells/mL)	Contrib. (%)	Avg. Abund (cells/mL)	Contrib. (%)
Fragilariopsis spp.	4	20	5	23	5	26
Unknown small pennates	4	10	2	8	2	7
Proboscia spp.	1	6	1	6	1	4
Pseudo-nitzschia spp.	1	4	2	6	2	10
Fragilariopsis pseudonana	11	4	2	7	0.89[A]	1[A]
Corethron spp.	1	3	1[A]	2[A]	0.40[A]	0.40[A]
Chaetoceros spp.	2	10	3	11	2	12
Coscinodiscus spp.	2	10	2	8	2	10
Unknown small centrics	1	8	1	5	1	2
Chaetoceros dichaeta	1	7	1	5	2	7
Dactyliosolen antarcticus	1	4	2	7	2	8
No. of species	16.50		16.90		15.10	
Abundance (cells/mL)	560.30		882.10		645.10	
Margalef d	2.60		2.37		2.23	
Pielou's J'	0.45		0.30		0.35	

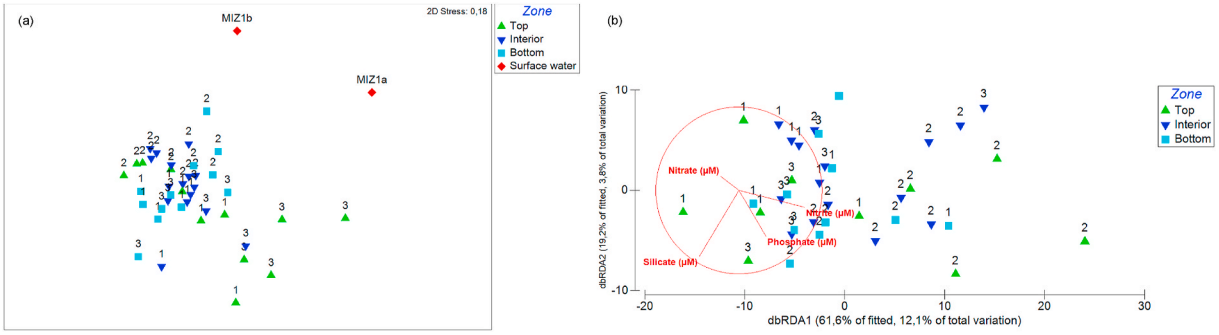

Fig. 6. (a) Multi-Dimensional Scale (MDS) analysis of sea-ice and surrounding surface water microalgae community structure and (b) Distance linear model (DistelM) of the relationship between nutrient concentrations and sea-ice algae biological community variation. Data were fourth-root transformed using the Bray Curtis similarity resemblance matrix. Numbers indicate the pancake samples (1, 2, and 3).

Table 3
Relationships between sympagic nutrient concentrations and sea-ice algae biomass (chlorophyll-a; Chl a) according to depth layer and on average for all samples (Spearman rank correlation coefficient).

Depth layer	Nutrients (µM)	Total Chl a (>0.3 µm)	Chl a (>2.7 µm)	Chl a (0.3–2.7 µm)
Top	NO_3^-	0.33	0.34	−0.24
	$Si(OH)_4$	0.55	0.60	−0.24
	NO2-	−0.03	0.13	−0.20
	$PO4^{3-}$	−0.47	−0.32	−0.10
Interior	NO_3^-	−0.19	−0.07	−0.72A
	$Si(OH)_4$	−0.42	−0.31	−0.75A
	NO2-	−0.54A	−0.48	−0.47
	$PO4^{3-}$	−0.12	−0.08	−0.07
Bottom	NO_3^-	0.18	0.20	−0.31
	$Si(OH)_4$	−0.12	−0.11	−0.24
	NO2-	−0.15	−0.12	0.64A
	$PO4^{3-}$	−0.51	−0.53	−0.35
All	NO_3^-	0.03	0.13	−0.55A
	$Si(OH)_4$	−0.15	−0.02	−0.50A
	NO2-	−0.27	−0.18	−0.14
	$PO4^{3-}$	−0.30	−0.24	−0.17

Significance shown at $p < 0.05$; marked as A.

sampling was 1:1.7. In the absence of biological activity, the N:$Si(OH)_4$ ratio within the ice would have been the same, which is not what we observed. Second, diatoms consume silicate and nitrate at a ratio of 1:1 when favorable environmental conditions persist (i.e., when iron is

Table 4
Relationships between sea-ice algae cell abundance and nutrient concentrations according to depth layer (Spearman rank correlation coefficient).

		NO_3^- (µM)	$Si(OH)_4$ (µM)	NO_2^- (µM)	PO_4^{3-} (µM)
Top	Total protist cells	−0.88[A]	−0.72 [A]	0.71 [A]	0.18
	Dinoflagellates	−0.42	−0.45	0.01	0.01
	Pennate diatoms	−0.89 [A]	−0.79	0.72 [A]	0.18
	Centric diatoms	−0.60	−0.45	0.71 [A]	0.27
	Silicoflagellates	−0.73 [A]	−0.66 [A]	0.66 [A]	−0.16
	Coccolithophores	−0.37	−0.09	0.48	0.24
	Ciliates	0.13	0.17	−0.33	0.10
Interior					
	Total protist cells	−0.39	−0.44	0.17	0.37
	Dinoflagellates	−0.03	0.25	0.24	−0.20
	Pennate diatoms	−0.39	−0.42	0.15	0.27
	Centric diatoms	−0.06	−0.03	0.26	0.45
	Silicoflagellates	−0.26	−0.35	0.14	0.53 [A]
	Coccolithophores	−0.06	0.10	0.10	0.18
	Ciliates	0.17	−0.08	−0.50 [A]	−0.03
Bottom					
	Total protist cells	−0.22	0.14	−0.25	−0.47
	Dinoflagellates	0.47	0.10	0.40	−0.10
	Pennate diatoms	−0.37	0.42	0.06	−0.59
	Centric diatoms	0.25	−0.59	−0.72 [A]	−0.22
	Silicoflagellates	0.19	0.04	−0.16	0.02
	Coccolithophores	−0.19	0.53	0.15	−0.39
	Ciliates	−0.07	0.76 [A]	0.60	−0.22

Significance shown at $p < 0.05$; marked as [A]

Table 5
Distance linear model output using R^2 function.

Nutrients (μM)	Sea-ice algae (cell/mL)	
	Marginal test	Sequential tests
	P	**P**
NO_3^-	0.11	0.12 [A]
$Si(OH)_4$	0.07	0.04 [A]
NO_2^-	0.00[A]	0.02 [A]
PO_4^{3-}	0.160	0.11

Significance shown at $p < 0.05$; marked as [A].

readily available; Hutchins and Bruland, 1998; Takeda, 1998) and increase their silicate-to-nitrate consumption ratio when iron is limiting (Franck et al., 2000; Brzezinski et al., 2003, 2015). Since sea ice is known to accumulate high concentrations of iron (Lannuzel et al., 2016), the measured 1:1 relationship between N and $Si(OH)_4$ may thus indicate elevated diatom activity. Third, despite being contained within the pancakes, the sea-ice algae would have experienced a more constant, and thus in net higher, supply of light than phytoplankton inhabiting the mixed layer, which is typically >100 m deep in the winter Antarctic Zone of the SO (Sallée et al., 2010). Fourth, silicate concentrations were on average higher in surface waters (47 μM) than in the sea-ice (34.4 μM). Depletion of the sea-ice silicate pool was likely the result of the large algal standing stock, dominated by diatoms (Fig. 5b) (Thomas and Dieckmann, 2002b). We conclude that the sea-ice phytoplankton community was actively growing at the time of sampling. Furthermore, the microscopy data show that this algal community was overwhelmingly dominated by diatoms, particularly pennate diatoms, which is indicative of a mature community (Leu et al., 2015; van Leeuwe et al., 2018).

The concentrations of all dissolved inorganic N (DIN) species (i.e., nitrate, nitrite, ammonium) were higher in the sea-ice than in surface waters (Fig. 3), likely due to active regeneration via the detritus-based microbial food web within the ice (Fripiat et al., 2015, 2017). Additionally, the nitrite concentrations and pennate diatom and dinoflagellate abundances were positively correlated, which may have resulted from regeneration processes related to the high sea-ice algae standing stock occurring coincident with the growth of the diatoms (i.e., the sea-ice nutrient paradox; Roukaerts et al., 2021). Sea-ice brine nitrate and ammonium concentrations as high as 121 μM and 48 μM, respectively, have been observed previously and attributed to cell lysis, algal mortality, inefficient grazing, and N remineralisation (Arrigo et al., 1995; Günther et al., 1999). In our study, the accumulation of ammonium to concentrations ranging from 3.0 to 7.7 μM in the ice (versus <1 μM in surface waters) can be explained by intense microbial remineralisation of organic matter in the sea-ice brine, in excess of the lower rate of ammonium assimilation. This decoupling between the rates of ammonium assimilation and microbial remineralisation may occur because autotrophic ammonium assimilation requires light while the microbial loop is not constrained by light availability (Fripiat et al., 2017).

The elevated nitrite and nitrate concentrations indicate that nitrification, the chemoautotrophic microbial oxidation of ammonium to nitrite and then nitrate, was also active in the winter sea-ice, as has been observed in the spring (Fripiat et al., 2014; Roukaerts et al., 2016). Indeed, Fripiat et al. (2014) concluded based on nitrate isotope measurements that in situ nitrification produced up to 70% of the nitrate assimilated by Antarctic pack-ice algae in spring. In our winter study, the sea-ice nitrate concentration was on average 7.5 μM higher than that of seawater. Additionally, the decline in the sea-ice silicate concentration suggests that 12.4 μM nitrate may have been coincidentally consumed by active sea-ice diatoms (i.e., assuming nitrate and silicate were consumed in a ratio of ~1:1, as implied by the slope of the relationship in Fig. 4a). Taken together, and assuming that the initial nitrate concentration in the sea-ice brine at the time of ice formation was similar to that in the underlying seawater (Fripiat et al., 2017), our observations suggest that nitrification produced ~20 μM nitrate since pancake formation. This scenario contradicts predictions, admittedly made based on very little data, that the early-winter sea-ice microbial community is near-dormant (Fripiat et al., 2017).

The sea-ice N:P ratios (average of 27.4:1) were higher than those expected for (and typically measured in) surface seawater (here, 13.4:1) (Redfield et al., 1963). SO diatoms are known to consume N and P in a fairly low ratio (10:1 to 14:1; Arrigo et al., 2002) compared to temperate species, which would leave the ambient nutrient pool enriched in N relative to P, as observed in this study (Weber and Deutsch, 2010). A similar dynamic may be at play within the sea-ice, with species-specific metabolic requirements, physiological response, life history, cell size, and distribution within the ice contributing to the high observed variability in the nutrient N:P ratio (Klausmeier et al., 2008; Weber and Deutsch, 2010; Lyon and Mock, 2014; Matsumoto et al., 2020). Additionally, while the remineralization and release of P from particulate organic matter is more rapid than that of N (Burkhardt et al., 2014), phosphate is also easily adsorbed by metal organic complexes, which removes it from solution (Becquevort et al., 2009; Lannuzel et al., 2011; Fripiat et al., 2017), potentially raising the N:P ratios in the ice. However, we observed a similar phosphate concentration in the sea-ice and surrounding seawater, such that we cannot confidently elucidate the relationship between phosphate and sea-ice biogeochemical cycling via the microbial loop or primary production in winter.

4.2. Size distribution of the sea-ice algae community

This study shows the clear dominance of the phytoplankton community by diatoms, primarily nano- and micro-sized diatoms (>2.7 μm), in both the sea-ice and the surrounding seawater. An abundance of large diatoms has previously been observed in newly formed sea-ice and attributed to accumulation during frazil ice formation (van Leeuwe et al., 2018). The dominance of larger cells could also imply a more established sea-ice community (e.g., Carnat et al., 2014; Carnat et al., 2016; Tison et al., 2017; Tison et al., 2020).

4.3. Microhabitats

A high abundance and biomass of sea-ice algae was observed throughout the sea-ice depth layers (Fig. 5). This is a common feature of Antarctic pack ice, with biological communities well-distributed throughout the ice (Torstensson et al., 2018). However, we found that the sea-ice algae community structure was significantly different among depth layers (top, interior, and bottom) in the pancakes. This depth-related variability likely indicates the existence of microhabitats that favour different species with specific preferences (Horner et al., 1992). Below, we examine the depth-distribution of sea-ice algae in our pancake samples.

4.3.1. Top layer

While pack-ice algae community studies, particularly of the surface versus interior assemblages, are sparse, the surface layer of Antarctic pack-ice has been shown to contain high sea-ice algae biomass, at least in spring through autumn, due to communities residing within the infiltration layers (Lizotte, 2003). In our study, however, biomass was generally lowest in the top layer of the pancakes. Sea-ice algae growth may have been restricted in this layer due to the passing of explosive cyclones across the study area, which exposed the upper column of sea-ice to rapid temperature changes (midlatitude warm oceanic air) and storm waves (Vichi et al., 2019). At the same time, disparate habitats were likely responsible for species accumulating to variable abundances throughout the pancakes. One example of this are the diatoms, *Corethron* spp. and *Dactyliosolen antarcticus*, that show a large and minor contribution, respectively, to community structure in the top and lower layers (Table 2).

4.3.2. Interior layer

Higher average total biomass and microalgae abundance was observed in the interior of all the pancakes compared to the top and bottom layers. Dense interior communities are usually a product of the heterogenous structure of Antarctic pack-ice, resulting from physical sea-ice processes such as aging, refreezing, and surface flooding (Ugalde et al., 2016; van Leeuwe et al., 2018). High biomass interior communities were found in pack ice in the Weddell Sea (AWECS 2013) observations that were explained by high sea-ice permeability resulting from warm cyclonic events and deep snow cover (Tison et al., 2017). However, the interior diffuse community described by Horner et al. (1992) for pack ice better characterizes our observations of the interior layer, since a similar sea-ice algae biomass concentration (<10 μg/L) and community assemblage (consisting of diatoms, dinoflagellates, ciliates, and coccolithophores) was observed. Furthermore, the significant relationship between ciliates and nutrients (negative correlation with nitrite and positive correlation with phosphate; Table 5) in this layer is consistent with active regeneration. Macronutrient regeneration is common in sea-ice (Dieckmann et al., 1991; Fripiat et al., 2015, 2017; Torstensson et al., 2018), controlled by sympagic biota such as bacteria, foraminifera, and other protozoa including ciliates (Dieckmann et al., 1991), with a potential contribution from biofilms (Roukaerts et al., 2021).

4.3.3. Bottom layer

We observed a significant correlation between increasing pico-sea-ice algae abundance and decreasing nitrite concentrations in the pancake bottom layers. Small algae tend to be reduced N specialists, with their high surface area-to-volume ratios providing them with an enhanced affinity for low concentrations of ammonium (Fawcett et al., 2011; Glibert et al., 2015 and references therein). This results in less ammonium being available for oxidation to nitrite. We further observed a higher accumulation of coccolithophores compared to other non-diatom groups in the bottom layer. While coccolithophores typically succeed (rather than co-exist in high abundance with) diatoms in the ocean (Margalef, 1978), the sea-ice environment, particularly the bottom layers of SO pancake ice, could provide a unique opportunity for diatom-coccolithophore coexistence where the physicochemical requirements for growth are met for both functional groups to proliferate simultaneously. Nissen et al. (2018) recently showed a significantly greater control of grazing on diatom versus coccolithophore abundance; if this top-down control is weaker in pancake ice than in the surface ocean, combined with the fact that other essential resources are generally more abundant in the ice, the result could be enhanced diatom-coccolithophore coexistence.

4.4. Algal biomass and community composition in surface waters and the sea-ice

Winter algae biomass was significantly higher in the sea-ice than in the surrounding seawater (Fig. 5a). Similarly low surface-water (<0.1 μg/L) and high sea-ice (>1 μg/L) chlorophyll-a concentrations were observed during the PIPERS study of the MIZ of the central and western Ross Sea during early winter (Tison et al., 2020). A chlorophyll-a concentration >1 μg/L is usually considered a bloom in the open ocean, which highlights the extreme concentration of biomass retained within the sea-ice during winter, reaching 5 μg/L in the sea-ice interior. Given this, and the nutrient dynamics discussed in section 4.1, we hypothesize that sea-ice algae were growing within the pancake ice during winter and were likely seeded from the surrounding surface water. This notion is supported by the lack of significant difference between sea-ice and the surrounding surface seawater in terms of both community structure and the number of species found. A strong overlap in species composition between pack-ice and the water column is often observed prior to and following ice-breakup and has been interpreted as resulting from the seeding effect of the surrounding water on the ice through scavenging (e.g., Kristiansen et al., 1998; Brierly and Thomas, 2002; Szymanski and Gradinger, 2016). Therefore, we suggest that our study site (Fig. 1) may be characterized as a closely coupled system during winter, similar to the Weddell Sea pack ice during late summer (Garrison et al., 1987). However, the coupling may not hold in other seasons (e.g., spring, early summer) as the sea-ice and surface water communities evolve separately.

4.5. Relationship between biogeochemical parameters and sea-ice algae community

We observed no limiting effect of macronutrients on the sea-ice algae community, since all nutrients were present at non-zero concentrations alongside high average total chlorophyll biomass (2.4 μg/L) in all pancakes. Consistent with a lack of nutrient limitation, the Distance Based Linear model (DistelM) revealed that the measured nutrients explained only 15.9% of the total variation in the sea-ice algae community structure, with nitrite and silicate emerging as the only significant drivers of community composition (Table 5). Macronutrients are not the only factors influencing phytoplankton growth, however, and it is likely that parameters not considered in our analysis, such as trace metal concentrations, light availability, and predation, also affected community structure.

We consider centric diatoms to have been relatively abundant in our study since their contribution to the community exceeded 10%, which is higher than that observed by Clarke and Ackley (1983), Meiners et al. (2016), and Hop et al. (2020). However, pennate diatoms were the dominant taxa in all sea-ice and surface water samples (Lizotte, 2001; Ugalde et al., 2016; van Leeuwe et al., 2018). This taxon often dominates under the ephemeral conditions of the MIZ, and in diatom sea-ice communities characterized by high abundances of the family *Bacillariaceae* (Garrison, 1991; Eicken, 1992; Torstensson et al., 2015). The dominant taxa identified in this study (Table 2) were similar to those observed in east Antarctic pack ice (Ugalde, 2015), east Antarctic sea-ice (Meiners et al., 2011), Ross Sea sea-ice (Tison et al., 2020), wintertime surface waters in the west Indian sector (Weir et al., 2020), and in the surface mixed layer of the eastern Indian sector of the SO in summer (Gomi et al., 2010). Although these studies focused on disparate temporal and spatial scales, it is evident that similar dominant phytoplankton taxa can be found in both surface waters and sea-ice in Antarctic waters.

Fragilariopsis spp. was the dominant pennate diatom genus across all depth layers of the pancakes. Species of this genus often dominate the sea-ice environment (Krell et al., 2008), including the pack ice (Lizotte, 2001), the open waters of the MIZ (Kang and Frexyll, 1992), and the winter mixed layer of the Antarctic Zone just north of the MIZ (Weir et al., 2020). Some species in this class are considered model psychrophilic organisms, adapted to extremely low temperatures and high brine salinities (Krell et al., 2008).

We enumerated low average abundances of dinoflagellates in all sea-ice samples compared to the ciliates, silicoflagellates, and coccolithophores. By contrast, using a sequencing approach, Torstensson et al. (2015) found that bottom sea-ice communities in mid-summer in the Amundsen and Ross Seas were dominated by dinoflagellates, which they attributed to the low light conditions encountered near the base of the ice. The lower dinoflagellate abundances observed in our study are difficult to explain by light availability since incident light in winter is far lower than that experienced by sea-ice algae in summer. Molecular methods of algal community analysis appear to generally yield higher abundances of sea-ice dinoflagellates than traditional microscopy (Gast et al., 2006; Bachy et al., 2011; Torstensson et al., 2015), a phenomenon that has been suggested (although not proven) to result from sea-ice processing methods such as thawing (as used in this study) (Garrison and Buck, 1982; Gast et al., 2006; Torstensson et al., 2015).

5. Concluding remarks

In this study, we provide the first evidence for the active growth of sea-ice algae in pancake ice during winter (July 2017) in the southern Indian MIZ of the SO. Our findings are similar to observations made in winter in the Ross Sea pack ice (2017, PIPERS) and Weddell Sea pack ice (2013, AWECS). We find that synoptic-scale weather events (i.e., explosive cyclones) and the pancake-ice life cycle exert considerable control over the physical sea-ice structure and its biogeochemical properties. Relationships observed between sea-ice protist functional groups and macronutrient concentrations and stoichiometry indicate i) a coalesced brine channel system characterized by elevated permeability, and ii) the presence of an active sea-ice algae community and microbial loop, with high rates of nitrogen regeneration inferred from elevated nitrate and ammonium concentrations. Our findings contradict a recent meta-study of pack-ice nutrient concentrations (Fripiat et al., 2017), which hypothesised that sea-ice algae are not active during winter in the Antarctic pack-ice. It is possible, however, that the northern reaches of the MIZ where our pancakes were collected are more dynamic and biologically active than the pack-ice given that light levels are higher and the ice is typically thinner. The biogeochemical functioning of the northern versus southern MIZ warrants further investigation. Additional work is also needed to identify the seasonal drivers of biological variations in the ice and underlying seawater, with implications for understanding how climate change will impact sea-ice algae communities, in terms of distribution, assemblage, and abundance, as well as carbon export potential and food supply to higher trophic levels.

Declaration of funding

This work was supported by the South African Departments of Forestry, Fisheries, and Environment (formerly Environmental Affairs) and Science and Innovation (DSI), and the National Research Foundation through the South African National Antarctic Program (grants 110735 and 129232 to S. Fawcett). S. Louw thanks the Department of Conservation and Marine Sciences at the Cape Peninsula University of Technology for financial support. S. Fawcett acknowledges an African Academy of Sciences/Royal Society FLAIR fellowship.

Declaration of competing interest

The authors declare that they have no known competing financial interests or personal relationships that could have appeared to influence the work reported in this paper.

Acknowledgements

We are grateful to Captain Knowledge Bengu and the crew of the R/V *SA Agulhas II*, as well as Chief Scientist, Marcello Vichi. S. Louw thanks the University of Cape Town's Oceanography and Engineering Departments, in particular Raquel Flynn and Hazel Little for continuous assistance in both data assimilation and analysis, and Shantelle Smith for ammonium concentration measurements. Thank you to Dr S. Fietz and Prof E. Campbell for their comments on an earlier version of this manuscript. The authors acknowledge the support of the DSI Biogeochemistry Research Infrastructure Platform (BIOGRIP). The data described in this manuscript are available at 10.5281/zenodo.5256078.

References

Alberello, A., Onorato, M., Bennetts, L., Vichi, M., Eayrs, C., MacHutchon, K., Toffoli, A., 2019. Brief communication: pancake ice floe size distribution during the winter expansion of the Antarctic marginal ice zone. Cryosphere 13, 41–48. https://doi.org/10.5194/tc-13-41-2019.

Anderson, M.J., Gorley, R.N., Clarke, K.R., 2008. PRIMER PERMANOVA +V6 (version 6). In: PERMANOVA+ for PRIMER: Guide to Software and Statistical Methods. PRIMER-E Ltd, Plymouth, UK.

Arrigo, K.R., Dieckmann, G.S., Gosselin, M., Robinson, D.H., Fritsen, C.H., Sullivan, C.W., 1995. High resolution study of the platelet ice ecosystem in McMurdo Sound, Antarctica: biomass, nutrient, and production profiles within a dense microalgal bloom. Mar. Ecol. Prog. Ser. 127, 255–268. https://doi.org/10.3354/meps127255.

Arrigo, K.R., Dunbar, R.B., Lizotte, M.P., Robinson, D.H., 2002. Taxon-specific differences in C/P and N/P drawdown for phytoplankton in the Ross Sea, Antarctica. Geophys. Res. Lett. 29 https://doi.org/10.1029/2002gl015277, 44.1-44.4.

Bachy, C., López-García, P., Vereshchaka, A., Moreira, D., 2011. Diversity and vertical distribution of microbial eukaryotes in the snow, sea ice and seawater near the north Pole at the end of the polar night. Front. Microbiol. 2 https://doi.org/10.3389/fmicb.2011.00106.

Becquevort, S., Dumont, I., Tison, J.-L., Lannuzel, D., Sauvée, M.L., Chou, L., Schoemann, V., 2009. Biogeochemistry and microbial community composition in sea ice and underlying seawater off East Antarctica during early spring. Polar Biol. 32, 879–895. https://doi.org/10.1007/s00300-009-0589-2.

Bouman, H.A., Lepère, C., Scanlan, D.J., Osvaldo, U., 2012. Phytoplankton community structure in a high-nutrient. low-chlorophyll region of the eastern Pacific Subantarctic region during winter-mixed and summer-stratified conditions. Deep-Sea Res. Pt. II 69, 1–11. https://doi.org/10.1016/j.dsr.2012.04.008.

Brierley, A.S., Thomas, D.N., 2002. Ecology of Southern Ocean pack ice. Adv. Mar. Biol. 43, 171–276. https://doi.org/10.1016/s0065-2881(02)43005-2.

Brzezinski, M.A., Dickson, M.-L., Nelson, D.M., Sambrotto, R., 2003. Ratios of Si, C and N uptake by microplankton in the Southern Ocean. Deep-Sea Res. Pt. II 50, 619–633. https://doi.org/10.1016/S0967-0645(02)00587-8.

Brzezinski, M.A., Krause, J.W., Bundy, R.M., Barbeau, K.A., Franks, P., Goericke, R., Landry, M.R., Stukel, M.R., 2015. Enhanced silica ballasting from iron stress sustains carbon export in a frontal zone within the California Current. J. Geophys. Res. Oceans 120, 4654–4669. https://doi.org/10.1002/2015JC010829.

Burkhardt, B.G., Watkins-Brandt, K.S., Defforey, D., Paytan, A., White, A.E., 2014. Remineralization of phytoplankton-derived organic matter by natural populations of heterotrophic bacteria. Mar. Chem. 163, 1–9. https://doi.org/10.1016/j.marchem.2014.03.007.

Carnat, G., Zhou, J., Papakyriakou, T., Delille, B., Goossens, T., Haskell, T., Schoemann, V., Fripiat, F., Rintala, J., Tison, J., 2014. Physical and biological controls on DMS,P dynamics in ice shelf-influenced fast ice during a winter-spring and a spring-summer transitions. J. Geophys. Res. Oceans 119, 2882–2905. https://doi.org/10.1002/2013JC009381.

Carnat, G., Brabant, F., Dumont, I., Vancoppenolle, M., Ackley, S., Fritsen, C., Delille, B., Tison, J., 2016. Influence of short-term synoptic events and snow depth on DMS, DMSP and DMSO dynamics in Antarctic spring ice. Elem. Sci. Anth. 4, 000135 https://doi.org/10.12952/journal.elementa.000135.

Chapman, C.C., Lea, M., Meyer, A., Sallée, J., Hindell, M., 2020. Defining Southern Ocean fronts and their influence on biological and physical processes in a changing climate. Nat. Clim. Change 10, 209–219. https://doi.org/10.1038/s41558-020-0705-4.

Clark, G.F., Stark, J.S., Johnston, E.L., Runcie, J.W., Goldsworthy, P.M., Raymond, B., Riddle, M.J., 2013. Light-driven tipping points in polar ecosystems. Global Change Biol. 19, 3749–3761.

Clarke, D.B., Ackley, S.F., 1983. Relative abundance of diatoms in Weddell Sea pack ice. Antarc. J. 181–182.

Clarke, K.R., Gorley, R.N., 2006. PRIMER v6 (Version 6). In: Primer v6: User Manual/Tutorial. PRIMER-E Ltd, Plymouth, UK.

Clarke, K.R., Warwick, R.M., 2001. Change in Marine Communities: an Approach to Statistical Analysis and Interpretation. PRIMER-E Ltd, Plymouth, UK.

Cota, G.F., Walker, S.O., Nelson, D.M., Muench, R.D., Gordon, L.I., 1992. Nutrient and biogenic particulate distributions, primary productivity and nitrogen uptake in the Weddell-Scotia Sea marginal ice zone during winter. J. Mar. Res. 50, 155–181.

Cox, G.F.N., Weeks, W.F., 1983. Equations for determining the gas and brine volumes in sea ice samples. J. Glaciol. 29, 306–316.

De Jong, H.B., Dunbar, R.B., Lyons, E.A., 2018. Late summer frazil ice-associated algal blooms around Antarctica. Geophys. Res. Lett. 45, 826–833. https://doi.org/10.1002/2017gl075472.

Delille, B., Vancoppenolle, M., Geilfus, N., Tilbrook, B., Lannuzel, D., Schoemann, V., Becquevort, S., Carnat, G., Delille, D., Lancelot, C., Chou, L., Dieckmann, G., Tison, J.-L., 2014. Southern Ocean CO2 sink: the contribution of the sea ice. J. Geophys. Res. Oceans 119, 6340–6355. https://doi.org/10.1002/2014jc009941.

Deppeler, S.L., Davidson, A.T., 2017. Southern Ocean phytoplankton in a changing climate. Front. Mar. Sci. 4 https://doi.org/10.3389/fmars.2017.00040.

Diamond, D., 1994. QuikChem Method 10-114-21-1-B: Silicate by Flow Injection Analysis. Lachat Instruments: Colorado).

Dieckmann, G.S., Lange, M.A., Ackley, S.F., Jennings, J.C., 1991. The nutrient status in sea ice of the Weddell Sea during winter: effects of sea ice texture and algae. Polar Biol. 11, 449–456. https://doi.org/10.1007/BF00233080.

Dodge, Y., 2008. The Concise Encyclopaedia of Statistics, first ed. Springer, New York, pp. 42–385.

Eicken, H., 1992. The role of sea ice in structuring Antarctic ecosystems. Polar Biol. 12, 3–13. https://doi.org/10.1007/978-3-642-77595-61.

Fawcett, S.E., Ward, B.B., 2011. Phytoplankton succession and nitrogen utilization during the development of an upwelling bloom. Mar. Ecol. Prog. Ser. 428, 13–31. https://doi.org/10.3354/meps09070.

Franck, V.M., Brzezinski, M.A., Coale, K.H., Nelson, D.M., 2000. Iron and silicic acid 1129 concentrations regulate Si uptake north and south of the polar frontal zone in the pacific 1130 sector of the Southern Ocean. Deep-Sea Res. Pt. II 47, 3315–3338. https://doi.org/10.1016/S0967-0645(00)00070-9.

Fripiat, F., Sigman, D.M., Fawcett, S.E., Rafter, P.A., Weigand, M.A., Tison, J.-L., 2014. New insights into sea-ice nitrogen biogeochemical dynamics from the nitrogen

isotopes. Global Biogeochem. Cycles 28, 115–130. https://doi.org/10.1002/2013GB004729.
Fripiat, F., Sigman, D.M., Massé, G., Tison, J.-L., 2015. High turnover rates indicated by changes in the fixed N forms and their stable isotopes in Antarctic landfast sea ice. J. Geophys. Res. 120, 3079–3097. https://doi.org/10.1002/2014JC010583.
Fripiat, F., Meiners, K.M., Vancoppenolle, M., Papadimitriou, S., Thomas, D.N., Ackley, S.F., Arrigo, K.R., Carnat, G., Cozzi, S., Delille, B., Dieckmann, G.S., Dunbar, R.B., Fransson, A., Kattner, G., Kennedy, H., Lannuzel, D., Munro, D.R., Nomura, D., Rintala, J.M., Schoemann, V., Stefels, J., Steiner, N., Tison, J.-L., 2017. Macro-nutrient concentrations in Antarctic pack ice: overall patterns and overlooked processes. Elem. Sci. Anth. 5, 13. https://doi.org/10.1525/elementa.217.
Frölicher, T.L., Sarmiento, J.L., Paynter, D.J., Dunne, J.P., Krasting, J.P., Winton, M., 2015. Dominance of the Southern Ocean in anthropogenic carbon and heat uptake in CMIP5 models. J. Clim. 28, 862–886. https://doi.org/10.1175/JCLI-D-14-00117.1.
Garrison, D.L., 1991. Antarctic sea-ice biota. Am. Zool. 31, 17–334. https://doi.org/10.1093/icb/31.1.17.
Garrison, D.L., Buck, K.R., 1982. Sea-ice algae in the Weddell Sea. Biomass distribution and the physical environment. EOS 63, 47.
Garrison, D.L., Buck, K.R., Fryxell, G.A., 1987. Algal assemblages in Antarctic pack ice and in ice-edge plankton. J. Phycol. 23, 564–572. https://doi.org/10.1111/j.1529-8817.1987.tb04206.x.
Gast, R.J., Moran, D.M., Beaudoin, D.J., Blythe, J.N., Dennett, M.R., Caron, D.A., 2006. Abundance of a novel dinoflagellate phylotype in the Ross Sea, Antarctica. J. Phycol. 42, 233–242. https://doi.org/10.1111/j.1529-8817.2006.00183.x.
Gleitz, M., Rutgers, V.D., Loeff, M., Thomas, D.N., Dieckmann, G.S., Millero, F.J., 1995. Comparison of summer and winter inorganic carbon, oxygen and nutrient concentrations in Antarctic sea ice brine. Mar. Chem. 51, 81–91.
Glibert, P., Wilkerson, F., Dugdale, R., Raven, J., Dupont, C., Leavitt, P., Parker, A., Burkholder, J., Kana, T., 2015. Pluses and minuses of ammonium and nitrate uptake and assimilation by phytoplankton and implications for productivity and community composition, with emphasis on nitrogen-enriched conditions. Limnol. Oceanogr. 61, 165–197. https://doi.org/10.1002/lno.10203.
Golden, K.M., Ackley, S.F., Lytle, V.I., 1998. The percolation phase transition in sea-ice. Science 18, 2238–2241. https://doi.org/10.1126/science.282.5397.2238.
Gomi, Y., Fukuchi, M., Taniguchi, A., 2010. Diatom assemblages at subsurface chlorophyll maximum layer in the eastern Indian sector of the Southern Ocean in summer. J. Plankton Res. 32, 1039–1050. https://doi.org/10.1093/plankt/fbq031.
Goto-Azuma, K.M., Hirabayashi, H., Motoyama, T., Miyake, T., Kuramoto, R., Uemura, M., Igarashi, Y., Iizuka, T., Sakurai, S., Horikawa, K., Suzuki, T., Suzuki, K., Fujita, Y., Kondo, S., Hattori, Fujii, Y., 2019. Reduced marine phytoplankton sulphur emissions in the Southern Ocean during the past seven glacials. Nat. Commun. 10, 3247. https://doi.org/10.1038/s41467-019-11128-6.
Grasshoff, K., 1976. Methods of Seawater Analysis, first ed. Verlag Chemie Weinheim, New York.
Grasshoff, K., Ehrhardt, M., Kremling, K., 1983. Methods of Seawater Analysis, second ed. Verlag Chemie Weinhein, New York.
Gruber, N., Landschützer, P., Lovenduski, M.-L., 2019. The variable Southern Ocean carbon sink. Ann. Rev. Mar. Sci 11, 159–186. https://doi.org/10.1126/sciadv.aav6471.
Günther, S., Gleitz, M., Dieckmann, G.S., 1999. Biogeochemistry of Antarctic sea ice: a case study on platelet ice at Drescher Inlet, Weddell Sea. Mar. Ecol. Prog. Ser. 177, 1–13. https://doi.org/10.3354/MEPS177001.
Hayek, L.-A.C., Buzas, M.A., 2013. On the proper and efficient use of diversity meusures with individual field samples. J. Foraminifer. Res. 43, 305–313. https://doi.org/10.2113/gsjfr.43.3.305.
Henley, S.F., Cavan, E.L., Fawcett, S.E., Kerr, R., Monteiro, T., Sherrell, R.M., Bowie, A. R., Boyd, P.W., Barnes, D.K.A., Schloss, I.R., Marshall, T., Flynn, R., Smith, S., 2020. Changing biogeochemistry of the Southern Ocean and its ecosystem implications. Front. Mar. Sci. 7 https://doi.org/10.3389/fmars.2020.00581.
Holmes, R.M., Aminot, A., Kérouel, R., Hooker, B.A., Peterson, B.J., 1999. A simple and precise method for 1142 measuring ammonium in marine and freshwater ecosystems. Can. J. Fish. Aquat. Sci. 56, 1801–1808.
Hoogstraten, A., Timmermans, K.R., de Baar, H.J.W., 2012. Morphological and physiological effects in *Proboscia alata* (*Bacillariophyceae*) grown under different light and CO2 conditions of the modern Southern Ocean. J. Phycol. 48, 559–568. https://doi.org/10.1111/j.1529-8817.2012.01148.x.
Hop, H., Vihtakari, M., Bluhm, B.A., Assmy, P., Poulin, M., Gradinger, R., Peeken, I., von Quillfeldt, C., Olsen, L.M., Zhitina, L., Melnikov, I.A., 2020. Changes in sea-ice protist diversity with declining sea ice in the Arctic Ocean from the 1980s to 2010s. Front. Mar. Sci. 7, 243. https://doi.org/10.3389/fmars.2020.00243.
Horner, R., Ackley, S.F., Dieckmann, G.S., Gulliksen, B., Hoshiai, T., Legendre, L., Melnikov, I.A., Reeburgh, W.S., Spindler, M., Sullivan, C.W., 1992. Ecology of sea ice biota. Habitat, terminology, and methodology. Polar Biol. 12, 417–427.
Hutchins, D.A., Bruland, K.W., 1998. Iron-limited diatom growth and Si:N uptake ratios in a coastal upwelling regime. Nature 393, 561–564. https://doi.org/10.1038/31203.
Instruments, Guildline, 1981. 'Autosal' Laboratory Salinometer Model 8400: Technical Manual. Guildline Instruments: Smiths Falls. Ontario Canada.
IPCC SROCC, 2019. In: Pörtner, H.-O., Roberts, D.C., Masson-Delmotte, V., Zhai, P., Tignor, M., Poloczanska, E., Mintenbeck, K., Alegría, A., Nicolai, M., Okem, A., Petzold, J., Rama, B., Weyer, N.M. (Eds.), IPCC Special Report on the Ocean and Cryosphere in a Changing Climate (in press).
Kang, S., Fryxell, G.A., 1992. *Fragilariopsis cylindrus* (Grunow) Krieger: the most abundant diatom in water column assemblages of Antarctic marginal ice-edge zones. Polar Biol. 12, 609–627. https://doi.org/10.1007/BF00236984.
Kang, S.-H., Kang, J.-S., Lee, S., Chung, K.H., Kim, D., Park, M.G., 2001. Antarctic phytoplankton assemblages in the marginal ice zone of the Northwestern Weddell Sea. J. Plankton Res. 23, 333–352. https://doi.org/10.1093/plankt/23.4.333.
Kettle, A.J., Andreae, M.O., Amouroux, D., Andreae, T.W., Bates, T.S., Berresheim, H., Bingemer, H., Boniforti, R., Curran, M.A.J., DiTullio, G.R., Helas, G., Jones, G.B., Keller, M.D., Kiene, R.P., Leck, C., Levasseur, M., Malin, G., Maspero, M., Matrai, P., McTaggart, A.R., Mihalopoulos, N., Nguyen, B.C., Novo, A., Putaud, J.P., Rapsomanikis, S., Roberts, G., Schebeske, G., Sharma, S., Simó, R., Staubes, R., Turner, S., Uher, G., 1999. A global database of sea surface dimethylsulfide (DMS) measurements and a procedure to predict sea surface DMS as a function of latitude, longitude, and month. Global Biogeochem. Cycles 13, 399–444. https://doi.org/10.1029/1999gb900004.
Klausmeier, C.A., Litchman, E., Daufresne, T., Levin, S.A., 2008. Phytoplankton stoichiometry. Ecol. Res. 23, 479–485. https://doi.org/10.1007/s11284-008-0470-8.
Kohlbach, D., Graeve, M., Lange, B.A., David, C., Schaafsma, F.L., van Franeker, J.A., Vortkamp, M., Brandt, A., Flores, H., 2018. Dependency of Antarctic zooplankton species on ice algae-produced carbon suggests a sea ice-driven pelagic ecosystem during winter. Global Change Biol. 24, 4667–4681. https://doi.org/10.1111/gcb.14392.
Krell, A., Beszteri, B., Dieckmann, G., Glöckner, G., Valentin, K., Mock, T., 2008. A new class of ice-binding proteins discovered in a salt-stress induced cDNA library of the psychrophilic diatom *Fragilariopsis cylindrus* (*Bacillariophyceae*). Eur. J. Phycol. 43, 423–433. https://doi.org/10.1080/09670260802348615.
Kristiansen, S., Farbrot, T., Kuosa, H., Myklestad, S.M., von Quillfeldt, C.H., 1998. Nitrogen uptake in the infiltration community, an ice algal community in Antarctic pack-ice. Polar Biol. 19, 307–315. https://doi.org/10.1007/s003000050251.
Lacour, T., Larivière, J., Babin, M., 2017. Growth, Chl a content, photosynthesis, and elemental composition in polar and temperate microalgae. Limnol. Oceanogr. 62, 43–58. https://doi.org/10.1002/lno.10369.
Lannuzel, D., Bowie, A.R., van der Merwe, P.C., Townsend, A.T., Schoemann, V., 2011. Distribution of dissolved and particulate metals in Antarctic sea ice. Mar. Chem. 124, 134–146. https://doi.org/10.1016/j.marchem.2011.01.004.
Lannuzel, D., Chever, F., van der Merwe, P.C., Janssens, J., Roukaerts, A., Cavagna, A.-J., Townsend, A.T., Bowie, A.R., Meiners, K.M., 2016. Iron biogeochemistry in Antarctic pack ice during SIPEX-2. Deep-Sea Res. Pt. II Top. Stud. Oceanogr. 131, 111–122. https://doi.org/10.1016/j.dsr2.2014.12.003.
Lazzara, L., Nardello, I., Ermanni, C., Mangoni, O., Saggiomo, V., 2007. Light environment and seasonal dynamics of microalgae in the annual sea ice at Terra Nova Bay, Ross Sea, Antarctica. Antarct. Sci. 19 https://doi.org/10.1017/s0954102007000119.
Leu, E., Mundy, C., Assmy, P., Campbell, K., Gabrielsen, T., Gosselin, M., Juul-Pedersen, T., Gradinger, R., 2015. Arctic spring awakening – steering principles behind the phenology of vernal ice algal blooms. Prog. Oceanogr. 139, 151–170. https://doi.org/10.1016/j.pocean.2015.07.012.
Lieblappen, R.M., Kumar, D.D., Pauls, S.D., Obbard, R.W., 2018. A network model for characterizing brine channels in sea ice. Cryosphere 12, 1013–1026. https://doi.org/10.5194/tc-12-1013-2018.
Lizotte, M., 2001. The contributions of sea-ice algae to Antarctic marine primary production. Am. Zool. 41, 57–73. https://doi.org/10.1093/icb/41.1.57.
Lizotte, M.P., 2003. The microbiology of sea ice. In: Thomas, D.N., Dieckmann, G.S. (Eds.), Sea Ice. Wiley-Blackwell, Oxford, pp. 184–210.
Lizotte, M.P., Sullivan, C.W., 1991. Photosynthesis-irradiance relationships in microalgae associated with Antarctic pack ice: evidence for in situ activity. Mar. Ecol. Prog. Ser. 71, 175–184.
Lyon, B.R., Mock, T., 2014. Polar microalgae: new approaches towards understanding adaptations to an extreme and changing environment. Biol. 3, 56–80. https://doi.org/10.3390/biology3010056.
Margalef, R., 1978. Life forms of phytoplankton as survival alternatives in an unstable environment. Oceanol. Acta 1, 493–509.
Matsumoto, M., Tanioka, T., Rickaby, R., 2020. Linkages between dynamic phytoplankton C:N:P and the ocean carbon cycle under climate change. Oceanography 33. https://doi.org/10.5670/oceanog.2020.203.
McMinn, A., 2017. Ice Acidification: a review of the effects of ocean acidification on sea ice microbial communities. Biogeosciences 14, 3927–3935. https://doi.org/10.5194/bg-2017-111.
Meiners, K.M., Norman, L., Granskog, M.A., Krell, A., Heil, P., Thomas, D.N., 2011. Physico-ecobiogeochemistry of East Antarctic pack ice during the winter-spring transition. Deep-Sea Res. Pt. II Top. Stud. Oceanogr. 58, 1172–1181. https://doi.org/10.1016/j.dsr2.2010.10.033.
Meiners, K.M., Golden, K.M., Heil, P., Lieser, J.L., Massom, R., Meyer, B., Williams, G.D., 2016. Introduction: SIPEX-2: a study of sea-ice physical, biogeochemical and ecosystem processes off East Antarctica during spring 2012. Deep-Sea Res. Pt. II Top. Stud. Oceanogr. 131, 1–6. https://doi.org/10.1016/j.dsr2.2016.06.010.
Morley, S., Abele, D., Barnes, D., Cárdenas, C., Cotté, C., Gutt, J., Henley, S., Höfer, J., Hughes, K., Martin, S., Moffat, C., Raphael, M., Stammerjohn, S., Suckling, C., Tulloch, V., Waller, C., Constable, A., 2020. Global drivers on Southern Ocean ecosystems: changing physical environments and anthropogenic pressures in an earth system. Front. Mar. Sci. 7 https://doi.org/10.3389/fmars.2020.547188.
Nair, A., Mohan, R., Manoj, M.C., Thamban, M., 2015. Glacial-interglacial variability in diatom abundance and valve size: implications for Southern Ocean paleoceanography. Paleoceanography 30, 1245–1260. https://doi.org/10.1002/2014pa002680.
Nissen, C., Vogt, M., Münnich, M., Gruber, N., Haumann, A.F., 2018. Factors controlling coccolithophore biogeography in the Southern Ocean. Biogeosciences 15, 6997–7024. https://doi.org/10.5194/bg-2018-157.

Núñez-Pons, L., Avila, C., Romano, G., Verde, C., Giordano, D., 2018. UV-protective compounds in marine organisms from the Southern Ocean. Mar. Drugs 16, 336. https://doi.org/10.3390/md16090336.

Papadimitriou, S., Thomas, D., Kennedy, H., Haas, C., Kuosa, H., Krell, A., Dieckmann, G., 2007. Biogeochemical composition of natural sea ice brines from the Weddell Sea during early austral summer. Limnol. Oceanogr. 52, 1809–1823. https://doi.org/10.2307/4502337.

Parkinson, C.L., 2019. A 40-y record reveals gradual Antarctic sea ice increases followed by decreases at rates far exceeding the rates seen in the Arctic, 201906556 Proc. Natl. Acad. Sci. Unit. States Am. 116, 14414–14423. https://doi.org/10.1073/pnas.1906556116.

Pinkerton, M., Boyd, P., Deppeler, S., Hayward, A., Höfer, J., Moreau, S., 2021. Evidence for the impact of climate change on primary producers in the Southern Ocean. Front. Ecol. Evol. 9 https://doi.org/10.3389/fevo.2021.592027.

Rackow, T., Danilov, S., Goessling, H.F., Hellmer, H.H., Sein, D.V., Semmler, T., Jung, T., 2020. Antarctic sea ice decline delayed well into the 21st century in a high-resolution climate projection. In: EGU General Assembly 2020, EGU2020-20837. https://doi.org/10.5194/egusphere-egu2020-20837. (Accessed 29 August 2021).

Redfield, A.C., Ketchum, B.H., Richards, F.A., 1963. The influence of organisms on the composition of seawater. In: Hill, M.N. (Ed.), The Sea. Interscience Publishers, New York, pp. 26–77.

Roukaerts, A., Cavagna, A.-J., Fripiat, F., Lannuzel, D., Meiners, K.M., Dehairs, F., 2016. Sea-ice algal primary production and nitrogen uptake rates off East Antarctica. Deep-Sea Res. Pt. II Top. Stud. Oceanogr. 131, 140–149. https://doi.org/10.1016/j.dsr2.2015.08.007.

Roukaerts, A., Deman, F., Van der Linden, F., Carnat, G., Bratkic, A., Moreau, S., Lannuzel, D., Dehairs, F., Delille, B., Tison, J., Fripiat, F., 2021. The biogeochemical role of a microbial biofilm in sea ice: Antarctic landfast sea ice as a case study. Elem. Sci. Anth. 9 https://doi.org/10.1525/elementa.2020.00134.

Sallée, J., Speer, K., Rintoul, S., 2010. Zonally asymmetric response of the Southern Ocean mixed-layer depth to the southern annular mode. Nat. Geosci. 3, 273–279. https://doi.org/10.1038/ngeo812.

Sambrotto, R., Buesseler, K.O., Moore, J.K., Hiscock, M.R., Dickson, M.-L., Barber, R.T., 2003. The effect of marginal ice-edge dynamics on production and export in the Southern Ocean along 170°W. Deep-Sea Res. Pt. II Top. Stud. Oceanogr. 50, 579–603. https://doi.org/10.1016/S0967-0645(02)00585-4.

Sarmiento, J.L., Toggweiler, J.R., 1984. A new model for the role of the oceans in determining atmospheric PCO2. Nature 308, 621–624. https://doi.org/10.1038/308621a0.

Saxberg, B.E.H., Kowalski, B.R., 1979. Generalized standard addition method. Anal. Chem. 51, 1031–1038. https://doi.org/10.1021/ac50043a059.

Scott, F.J., Marchant, H.J., 2005. Antarctic Marine Protists. Australian Biological Resources Study, Canberra.

Siegenthaler, U., Wenk, T., 1984. Rapid atmospheric CO2 variations and ocean circulation. Nature 308, 624–626. https://doi.org/10.1038/308624a0.

Skatulla, S., Audh, R.R., Cook, A., Hepworth, E., Johnson, S., Lupascu, D.C., MacHutchon, K., Marquart, R., Mielke, T., Omatuku, E., Paul, F., Rampai, T., Schröder, J., Schwarz, C., Vichi, M., 2021. Physical and mechanical properties of winter first-year ice in the Antarctic marginal ice zone along the Good Hope Line. Cryosphere Discuss. https://doi.org/10.5194/tc-2021-209 (In review).

Smith, S., Altieri, K., Mdutyana, M., Walker, D., Parrott, R., Spence, K., Burger, J., Fawcett, S., 2021. Biogeochemical controls on wintertime ammonium accumulation in the surface layer of the Southern Ocean. Biogeosci. Discuss. https://doi.org/10.5194/bg-2021-149. In review.

Szymanski, A., Gradinger, R., 2016. The diversity. abundance and fate of ice algae and phytoplankton in the Bering Sea. Polar Biol. 39, 309–325. https://doi.org/10.1007/s00300-015-1783-z.

Takeda, S., 1998. Influence of iron availability on nutrient consumption ratio of diatoms in oceanic waters. Nature 393, 774–777. https://doi.org/10.1038/31674.

Taylor, B.W., Keep, C.F., Hall, R.O., Koch, B.J., Tronstad, L.M., Flecker, A.S., Ulseth, A.J., 2007. Improving the fluorometric ammonium method: matrix effects, background fluorescence, and standard additions. J. North Am. Benthol. Soc. 26, 167–177. https://doi.org/10.1899/0887-3593 (2007)26[167:itfamm]2.0.co.

Thomas, D.N., Dieckmann, G.S., 2002a. Biogeochemistry of Antarctic sea ice. Oceanogr. Mar. Biol. 40, 143–169. https://doi.org/10.1201/9780203180594.ch3.

Thomas, D.N., Dieckmann, G.S., 2002b. Antarctic sea ice - a habitat for extremophiles. Science 295, 641–644. https://doi.org/10.1126/science.1063391.

Tison, J.-L., Schwegmann, S., Dieckmann, G., Rintala, J., Meyer, H., Moreau, S., Vancoppenolle, M., Nomura, D., Engberg, S., Blomster, L., Hendricks, S., Uhlig, C., Luhtanen, A., de Jong, J., Janssens, J., Carnat, G., Zhou, J., Delille, B., 2017. Biogeochemical impact of snow cover and cyclonic intrusions on the winter Weddell Sea ice pack. J. Geophys. Res. Oceans 122, 9548–9571. https://doi.org/10.1002/2017jc013288.

Tison, J., Maksym, T., Fraser, A., Corkill, M., Kimura, N., Nosaka, Y., Nomura, D., Vancoppenolle, M., Ackley, S., Stammerjohn, S., Wauthy, S., Van der Linden, F., Carnat, G., Sapart, C., de Jong, J., Fripiat, F., Delille, B., 2020. Physical and biological properties of early winter Antarctic sea ice in the Ross Sea. Ann. Glaciol. 1–19. https://doi.org/10.1017/aog.2020.43.

Torstensson, A., Dinasquet, J., Chierici, M., Fransson, A., Riemann, L., Wulff, A., 2015. Physicochemical control of bacterial and protist community composition and diversity in Antarctic sea ice. Environ. Microbiol. 17, 3869–3881. https://doi.org/10.1111/1462-2920.12865.

Torstensson, A., Fransson, A., Currie, K., Wulff, A., Chierici, M., 2018. Microalgal photophysiology and macronutrient distribution in summer sea ice in the Amundsen and Ross Seas, Antarctica. PLoS One 13, 1–20. https://doi.org/10.1371/journal.pone.0195587.

Tréguer, P., Bowler, C., Moriceau, B., Dutkiewicz, S., Gehlen, M., Aumont, O., Bittner, L., Dugdale, R., Finkel, Z., Iudicone, D., Jahn, O., Guidi, L., Lasbleiz, M., Leblanc, K., Levy, M., Pondaven, P., 2018. Influence of diatom diversity on the ocean biological carbon pump. Nat. Geosci. 11, 27–37. https://doi.org/10.1038/s41561-017-0028-x.

Ugalde, S.C., 2015. Antarctic Sea Ice Algae: Primary Production and Carbon Allocation. PhD thesis. University of Tasmania, Tasmania.

Ugalde, S.C., Westwood, K.J., van den Enden, R., McMinn, A., Meiners, K.M., 2016. Characteristics and primary productivity of East Antarctic pack ice during the winter-spring transition. Deep-Sea Res. Pt. II Top. Stud. Oceanogr. 131, 123–139. https://doi.org/10.1016/j.dsr2.2015.12.013.

UNESCO, 1978. Eighth report of the joint panel on oceanographic tables and standards. In: UNESCO Technical Papers in Marine Science, pp. 28–35.

Utermöhl, H., 1931. Neue Wege in der quantitativen Erfassung des Planktons. (Mit besondere Beriicksichtigung des Ultraplanktons). Verh. Int. Verein. Theor. Angew. Limnol. 5, 567–595. https://doi.org/10.1080/03680770.1931.11898492.

van Leeuwe, M., Tedesco, L., Arrigo, K., Assmy, P., Campbell, K., Meiners, K., Rintala, J., Selz, V., Thomas, D., Stefels, J., Deming, J., 2018. Microalgal community structure and primary production in Arctic and Antarctic sea ice: a synthesis. Elem. Sci. Anth. 6, 4. https://doi.org/10.1525/elementa.267.

Vancoppenolle, M., Goosse, H., de Montety, A., Fichefet, T., Tremblay, B., Tison, J.-L., 2010. Modeling brine and nutrient dynamics in Antarctic sea-ice: the case of dissolved silica. *J.* Geophys. Res. Oceans 115, C02005. https://doi.org/10.1029/2009JC005369.

Vichi, M., Eayrs, C., Alberello, A., Bekker, A., Bennetts, L., Holland, D., de Jongh, E., Joubert, W., MacHutchon, K., Messori, G., Mojica, J.F., Onorato, M., Saunders, C., Skatulla, S., Toffoli, A., 2019. Effects of an explosive polar cyclone crossing the Antarctic marginal ice zone. Geophys. Res. Lett. 46, 5948–5958. https://doi.org/10.1029/2019gl082457.

Volk, T., Hoffert, M., 1985. Ocean carbon pumps: analysis of relative strengths and efficiencies in ocean-driven atmospheric CO2 changes. In: Sundquist, E., Broecker, W.S. (Eds.), The Carbon Cycle and Atmospheric OC2: Natural Variations Archean to Present. AGU, Washington, pp. 99–110.

Weber, T.S., Deutsch, C., 2010. Ocean nutrient ratios governed by plankton biogeography. Nature 467, 550–554. https://doi.org/10.1038/nature09403.

Weir, I., Fawcett, S.E., Smith, S., Walker, D., Bornman, T., Fietz, S., 2020. Winter biogenic silica and diatom distributions in the Indian sector of the Southern Ocean. Deep-Sea Res. Pt I: Oceanogr. Res. Papers 166. https://doi.org/10.1016/j.dsr.2020.103421.

Welschmeyer, N.A., 1994. Fluorometric analysis of chlorophyll-a in the presence of chlorophyll b and pheopigments. Limnol. Oceanogr. 39, 1985–1992. https://doi.org/10.4319/lo.1994.39.8.1985.

Wetzel, R.G., 2001. Limnology: Lake and River Ecosystems, third ed. Academic Press, San Diego.

Yoshida, K., Seger, A., Kennedy, F., McMinn, A., Suzuki, K., 2020. Freezing, melting and light stress on the photophysiology of ice algae: ex situ incubation of the ice algal diatom *Fragilariopsis cylindrus (Bacillariophyceae)* using an ice tank. J. Phycol. 56, 1323–1338. https://doi.org/10.1111/jpy.13036.